Maria L. Lacal
Senior Vice President, Nuclear
Regulatory & Oversight

Palo Verde
Nuclear Generating Station
P.O. Box 52034
Phoenix, AZ 85072
Mail Station 7605
Tel 623.393.6491

102-07380-MLL/MDD
December 1, 2016

ATTN: Document Control Desk
U.S. Nuclear Regulatory Commission
11555 Rockville Pike
Rockville, MD 20852

Dear Sirs:

Subject: **Palo Verde Nuclear Generating Station (PVNGS)**
Units 1, 2, and 3
Docket Nos. STN 50-528, 50-529, and 50-530
Addendum to Supplemental Response to NRC Generic Letter 2004-02, *Potential Impact of Debris Blockage on Emergency Recirculation during Design Basis Accidents at Pressurized-Water Reactors*

NRC Generic Letter (GL) 2004-02, *Potential Impact of Debris Blockage on Emergency Recirculation during Design Basis Accidents at Pressurized-Water Reactors,* requested licensees provide information on actions taken and analyses performed to address the potential impact of debris blockage on emergency recirculation during design basis accidents. To address this issue, Arizona Public Service Company (APS) has replaced the emergency core cooling system (ECCS) sump strainers in all three units of the Palo Verde Nuclear Power Station (PVNGS) with larger strainers of improved design.

In letter 102-06805, dated December 18, 2013, APS provided an updated response to the Generic Letter [Agencywide Document Access and Management System (ADAMS) Accession Number ML13357A218].

In April 2015, during drawing reviews for a separate engineering effort, encapsulated Microtherm insulation was identified on the reactor vessel of each PVNGS unit. Extent of condition efforts (drawing reviews and physical inspections) identified additional Temp-Mat insulation. These items had not been addressed in the APS updated response to Generic Letter 2004-02. These discovery items were captured in the PVNGS corrective action program.

Public teleconferences between APS and the NRC staff have been held to describe the efforts to address the discovery items (ADAMS Accession Numbers ML15239B322, ML15156B352, ML15268A131, ML15236A134, ML15328A379, ML15348A054 and ML16253A411).

A116
NRR

Engineering evaluations have been completed to address the discovery items that will remain part of the PVNGS design. APS is providing an addendum to the response to GL 2004-02 in the Enclosure to this letter.

Commitments are being made to the NRC by this letter as described in Section 3.4 of the Enclosure. Specifically, for each PVNGS Unit, a commitment is made to remove discrepant (i.e., not evaluated) fibrous insulation over the next two refueling outages for each Unit, beginning with the completed Fall 2016 Unit 3 refueling outage (3R19).

Should you need further information regarding this response, please contact Michael D. DiLorenzo, Licensing Section Leader, at (623) 393-3495.

I declare under penalty of perjury that the foregoing is true and correct.

Executed on December 1, 2016
(Date)

Sincerely,

Enclosure:

Addendum to Supplemental Response to NRC Generic Letter (GL) 2004-02, Revision 2

MLL/MDD/af

cc:	K. M. Kennedy	NRC Region IV Regional Administrator
	S. P. Lingam	NRC NRR Project Manager for PVNGS
	M. M. Watford	NRC NRR Project Manager
	C. A. Peabody	NRC Senior Resident Inspector for PVNGS

Enclosure

Addendum to Supplemental Response to NRC Generic Letter (GL) 2004-02, Revision 2

TABLE OF CONTENTS

LIST OF TABLES

LIST OF FIGURES

ACRONYMS	
AISC	American Institute of Steel Construction
ANSI/ANS	American National Standards Institute / American Nuclear Society
AoR	Analysis-of-Record
APS	Arizona Public Service Company
ASME	American Society of Mechanical Engineers
B&PV	Boiler and Pressure Vessel
BWROG	Boiling Water Reactor Owners Group
CCI	Control Components, Inc.
CFD	Computational Fluid Dynamics
CL	Cold Leg
CS	Containment Spray
CSS	Containment Spray System
DEGB	Double-ended Guillotine Break
DMWO	Design Master Work Order
ECCS	Emergency Core Cooling System
EWR	Engineering Work Request
GL 2004-02	Generic Letter 2004-02
GSI–191	Generic Safety Issue 191
HL	Hot Leg
HPSI	High Pressure Safety Injection
ICI	In-Core Instrumentation
LDFG	Low Density Fiber Glass
LOCA	Loss of Coolant Accident
LPSI	Low Pressure Safety Injection
NEI	Nuclear Energy Institute
NPSH	Net Positive Suction Head
NRC	Nuclear Regulatory Commission
PVNGS	Palo Verde Nuclear Generating Station
PWR	Pressurized Water Reactor
PWROG	Pressurized Water Reactor Owners Group
RAS	Recirculation Actuation Signal
RCP	Reactor Coolant Pump
RCS	Reactor Coolant System
RMI	Reflective-Metal Insulation
RPV	Reactor Pressure Vessel
RTD	Resistance-Temperature Detector
RWT	Refueling Water Tank
S&L	Sargent & Lundy, L.L.C.
SIAS	Safety Injection Actuation Signal
SSE	Safe Shutdown Earthquake

ACRONYMS	
TKE	Turbulent Kinetic Energy
ToR	Test-of-Record
UFSAR	Updated Final Safety Analysis Report
URG	Utility Resolution Guide
WC	Water Column
ZOI	Zone of Influence

1. Introduction

1.1 Background

On December 18, 2013, Arizona Public Service Company (APS) submitted Revision 2 to the supplemental response to Generic Letter (GL) 2004-02, *Palo Verde Nuclear Generating Station (PVNGS) Units 1, 2, and 3, Docket Nos. STN 50-528, 50-529, and 50-530, Revision 2 to Supplemental Response to NRC Generic Letter 2004 02, "Potential Impact of Debris Blockage on Emergency Recirculation During Design Basis Accidents at Pressurized-Water Reactors"* (ADAMS Accession Number ML13357A218) [1].

On April 15, 2015, APS documented discovery of Microtherm insulation on the Reactor Pressure Vessel (RPV) in all three Palo Verde Units. The newly-discovered Microtherm insulation on the RPV was not included in the analysis or testing upon which APS based Revision 2 to the supplemental response to GL 2004-02. APS entered this condition into the corrective action program [2].

On June 10, 2015, APS and the NRC staff held a public teleconference to discuss the recently discovered Microtherm. The meeting summary and APS presentation slides are available as ADAMS Accession Numbers ML15239B322 [3] and ML15156B352 [4], respectively. During this meeting, APS described that in addition to Microtherm, Temp-Mat insulation was discovered at several locations in the D-ring Steam Generator sub-compartments, the Reactor Coolant System (RCS) pipe penetrations through the concrete biological shield wall surrounding the RPV and in the Reactor Cavity. As was the case with Microtherm, newly-discovered Temp-Mat insulation was not included in the analysis or testing upon which Revision 2 to the supplemental response to GL 2004-02 was based.

On August 26, 2015, APS and the NRC staff held a public teleconference. At the meeting, APS stated its plan to pursue a combined strategy of (a) removal of selected portions of newly-discovered Temp-Mat and (b) justifying the remaining configuration, including Microtherm, using further evaluation. The meeting summary and the APS presentation slides are available as ADAMS Accession Numbers ML15268A131 [5] and ML15236A134 [6], respectively.

On December 17, 2015, APS and the NRC staff held a public teleconference to discuss progress and preliminary results of APS actions towards addressing the newly-discovered Microtherm and Temp-Mat insulation that had been discussed in previous meetings. The meeting notice and agenda, are available as ADAMS Accession Number ML15328A379 [7]. APS presentation slides are available as ADAMS Accession Number ML15348A054 [8]. During this meeting APS stated that an Addendum to Revision 2 to the Supplemental Response to GL 2004-02 would be provided.

On September 7, 2016, APS and the NRC staff held a public teleconference to discuss the current status of inspection activities and analysis results. The meeting slides are available as ADAMS Accession Number ML16253A411 [9].

1.2 Purpose

This document comprises an Addendum to Revision 2 to the Supplemental Response to GL 2004-02 [10]. The purpose of this document is to describe the conditions and actions that occurred after submittal of Revision 2 to the supplemental response to GL 2004-02, and provide

a basis for concluding that the configuration that will exist after all actions are complete is acceptable.

Section 2 provides a detailed description of the condition being addressed in this document.

Section 3 describes the means by which the condition is resolved, and contains a revised *Executive Summary* (Sub-section 3.2), a revised *Overall Compliance* Section (Sub-section 3.3), a revised *General Description and Schedule for Corrective Actions* Section (Sub-section 3.4) and a *Revised Strainer Structural Capacity Discussion* (Sub-section 3.5).

Section 4 provides the technical basis for establishing that the objectives of GL 2004-02 are satisfied.

2 Description of Condition

2.1 Microtherm

Figure 2-1 illustrates the scope of Microtherm insulation on the RPV. Microtherm insulation on the RPV is limited to a region at the RPV nozzles and four locations at 90-degrees apart on the RPV bottom head. The total volume of Microtherm insulation on the RPV is 83.4 ft^3 [11].

Figure 2-1: Microtherm Insulation on RPV

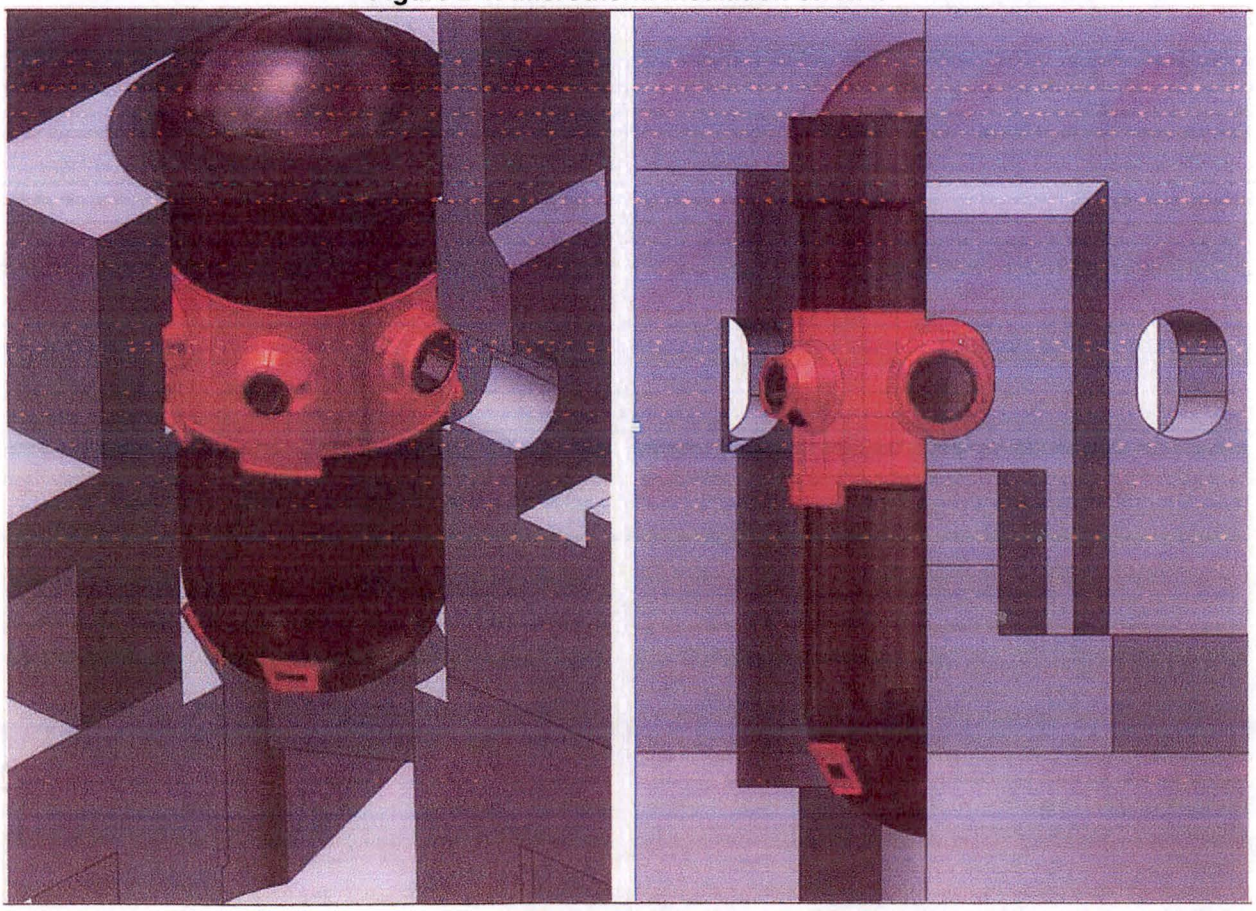

2.2 Temp-Mat

Figure 2-2 illustrates the scope of Temp-Mat insulation located in the nozzle region of the RPV, in the RCS pipe penetration through the concrete biological shield wall surrounding the RPV, and in the D-ring Steam Generator sub-compartment.

Gold-circled Temp-Mat items occur in Unit 3 only; other items occur in all three units.

Red-colored items affect pipe breaks in the D-ring Steam Generator sub-compartment; green-colored items affect pipe breaks at RPV nozzles.

During the walkdown of the installed configuration in Unit 1 during the Spring 2016 outage, additional Temp-Mat insulation blankets were identified between Reflective Metal Insulation (RMI) cassettes in a limited number of locations. These Temp-Mat blankets were removed, or will be removed, as described in Sections 3.1 and 3.4.

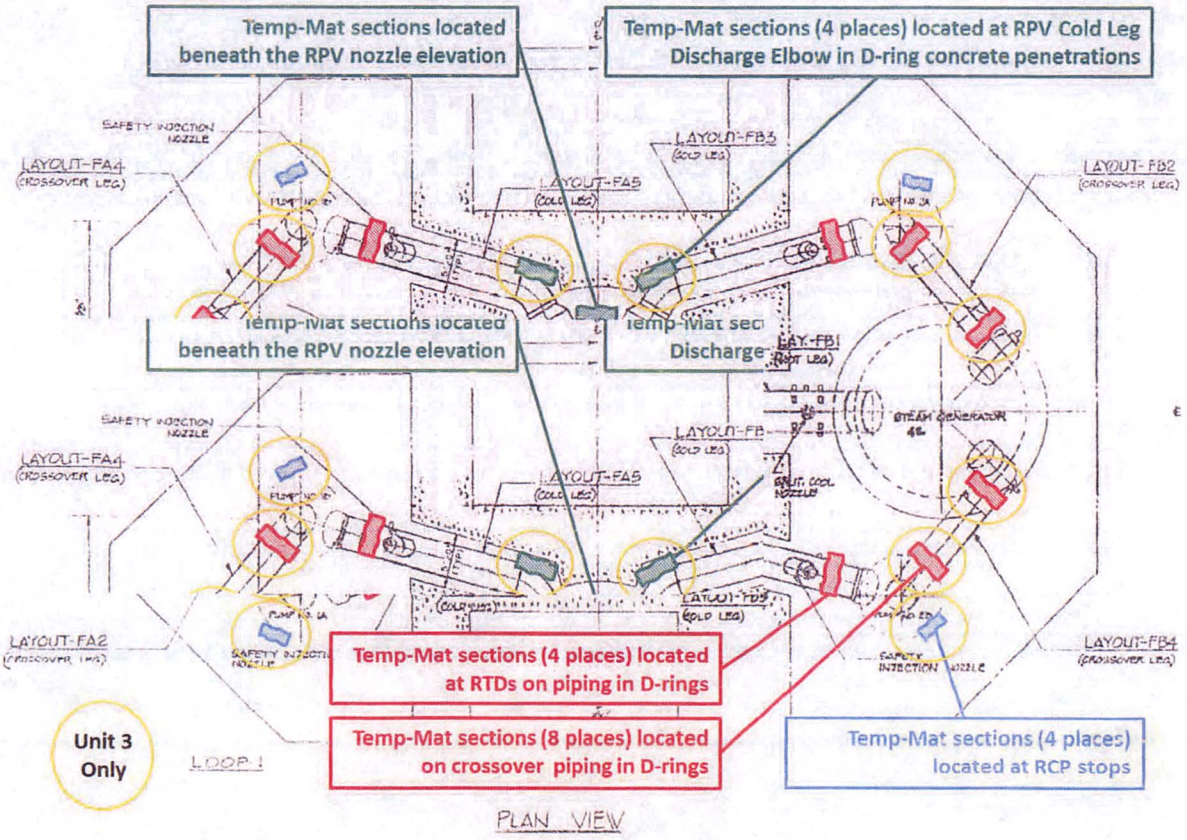

Figure 2-2: Temp-Mat at RPV Nozzle Region and In D-ring

Not shown in Figure 2-2 is Nukon insulation on Feedwater piping outside the bioshield wall, discussed in Section 2.3.

Figure 2-3 shows the locations of Temp-Mat in the region of the bottom of the RPV and the arrangement of Temp-Mat in the region.

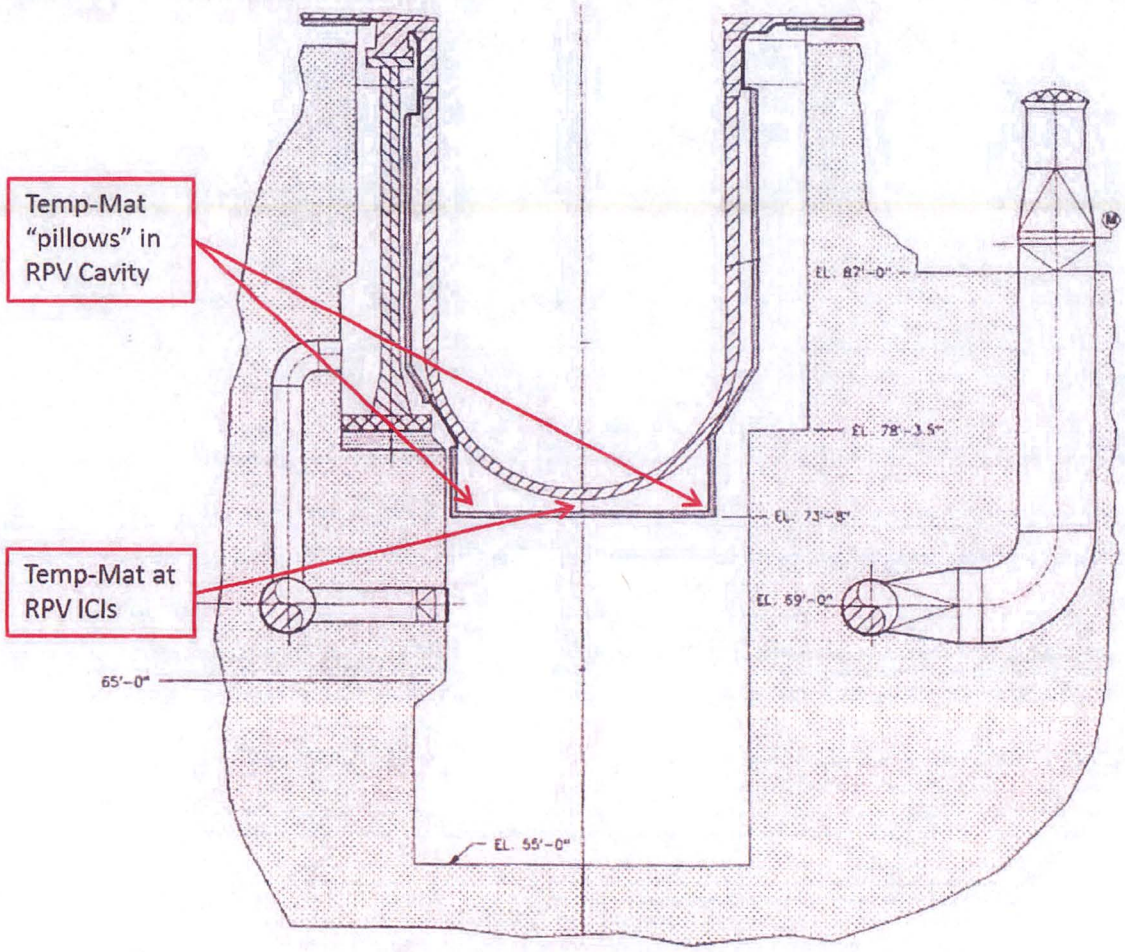

Figure 2-3: Temp-Mat Locations Below RPV

Table 2-1 provides a listing of Temp-Mat discovered after Revision 2 to the supplemental response to GL 2004-02 was submitted, that will not be removed and is evaluated in Section 4.

Table 2-1: Total Temp-Mat

Temp-Mat Location	Reference Figure	Units	QTY[1]
RPV Nozzle Region	Figure 2-2	1, 2 and 3	2.8
"Pillows" in RPV Cavity	Figure 2-3	1, 2 and 3	6.8
In-Core Instrumentation (ICIs) in RPV Cavity	Figure 2-3	1, 2 and 3	1.8

Note:
1. All quantities in ft^3 units

In addition to the Temp-Mat listed in Table 2-1, which will not be removed and is evaluated in Section 4, the Microtherm illustrated in Figure 2-1 will not be removed and is evaluated in Section 4.

2.3 Nukon

During the Fall 2015 Unit 2 refueling outage it was determined that some Nukon insulation on piping outside the bioshield wall, although originally identified in plant walkdowns, was not included for potential contribution to chemical effects in the Analysis of Record (AoR). The determination is documented in Engineering Evaluation ENG WO number 4719679 [12]. It was determined that Nukon insulation on piping outside the bioshield wall is not within the Zone of Influence (ZOI) of any pipe breaks and, therefore, will not contribute to strainer debris load. However, since this Nukon insulation on piping outside the bioshield wall is below the flood level, (i.e., can be submerged), it has been determined that it could contribute to chemical effects in the post-Loss of Coolant Accident (LOCA) recirculation pool. The Nukon insulation has or will be removed, as described in Table 3-1.

3 Overview of Condition Resolution Approach

3.1 Actions that APS Has or Intends to Implement

Two approaches are used to address the condition with newly-discovered Microtherm, Temp-Mat and the Nukon that was not considered in the chemical effects AoR. These are (1) remove the insulation, or (2) analytically demonstrate that acceptance criteria are satisfied. Table 3-1 shows the approach that is assigned to each insulation type at each location.

Table 3-1: APS Resolution Approach

Insulation Type	Location	Units Affected	Reference Figure	Resolution	Schedule
Microtherm	RPV Nozzle region	1, 2 and 3	Figure 2-1	Analytical Acceptance	n/a
Microtherm	RPV Bottom Head	1, 2 and 3	Figure 2-1	Analytical Acceptance	n/a
Temp-Mat	RCS Piping in D-ring (Crossover)	3 only	Figure 2-2	Removal	Completed Fall 2016
Temp-Mat	RPV Cold Leg Discharge Elbow	3 only	Figure 2-2	Determined to be RMI and reinstalled	Completed Fall 2016
Temp-Mat	RCS Piping in D-ring (Cold Leg at RTDs)	1	Figure 2-2	Removal	Completed Spring 2016
Temp-Mat	RCS Piping in D-ring (Cold Leg at RTDs)	2	Figure 2-2	Removal	Completed Fall 2015
Temp-Mat	RCS Piping in D-ring (Cold Leg at RTDs)	3	Figure 2-2	Removal	Completed Fall 2016
Temp-Mat	RCP Stops	3 only	Figure 2-2	Removal	Completed Fall 2016

Insulation Type	Location	Units Affected	Reference Figure	Resolution	Schedule
Temp-Mat	Beneath the RPV Nozzle Region	1, 2 and 3	Figure 2-2	Analytical Acceptance	n/a
Temp-Mat	"Pillows" in RPV Cavity	1, 2 and 3	Figure 2-3	Analytical Acceptance	n/a
Temp-Mat	ICIs in RPV Cavity	1, 2 and 3	Figure 2-3	Analytical Acceptance	n/a
Temp-Mat	Various discrepant insulation located inside Containment	1, 2 and 3	n/a	Removal	Second outage for each Unit, beginning with 3R19, Fall 2016
Nukon	80 ft of Containment	1	n/a	Removal for margin	Completed Spring 2016
Nukon	80 ft of Containment	2	n/a	Removal for margin	U2R20 - Spring 2017
Nukon	80 ft of Containment	3	n/a	Removal for margin	Completed Fall 2016

3.2 Revised Executive Summary

The following is the updated version of the complete *Executive Summary* that was provided in Revision 2 of the APS Supplemental Response to GL 2004-02.[1]

In response to research relative to sump-strainer clogging, the U.S. Nuclear Regulatory Commission (NRC) opened Generic Safety Issue (GSI) - 191, *Assessment of Debris Accumulation on Pressurized Water Reactor (PWR) Sump Performance*. The objective of GSI-191 is to ensure that post-accident debris blockage does not impede or prevent operation of the Emergency Core Cooling System (ECCS) or Containment Spray System (CSS) in recirculation mode at pressurized water reactors (PWRs) during accidents for which recirculation is required.

Based on information identified during the efforts to resolve GSI-191, the NRC Staff determined that the previous guidance used to develop current licensing basis analyses did not adequately and completely model sump screen debris blockage and related effects. As a result, the NRC Staff revised the guidance for determining PWR recirculation sump screen susceptibility to the adverse effects of debris blockage and issued Generic Letter (GL) 2004-02. GL 2004-02 requests that addressees (NRC licensees that operate PWRs) perform new, more realistic analyses and submit information to the NRC confirming the functionality of the ECCS during design basis accidents that require recirculation operations.

[1]References cited in this Section using [Ref. X.Y] format refer to references provided in Revision 2 of the APS Supplemental Response to GL 2004-02, not this Addendum. References cited using the format [X] are specific to this Addendum and are listed in the References Section of this document.

Arizona Public Service Company (APS) Letter 102-05336, dated September 1, 2005, provided the Palo Verde Nuclear Generating Station (PVNGS) initial written response to the NRC, per GL 2004-02 Request No. 2 [Ref. 4.90]. APS submitted a Supplemental Response to GL 2004-02 on February 29, 2008 [Ref. 4.91] and a revised Supplemental Response to GL 2004-02 on March 13, 2009 [Ref. 4.113]. However, the 2009 Supplemental Response did not address in-vessel effects, because that information was not available.

In-vessel fuel effects may be resolved either with the NRC safety evaluation for WCAP-16793-NP, Revision 2, (Issued on April 8, 2013) or upon completion of WCAP-17788. APS submitted a letter [Ref. 4.125] to the NRC in which Option 2A (deterministic), *Mitigative Measures and Alternative Methods Approach,* from SECY-12-0093 [Ref. 4.126] was chosen for GSI-191 resolution. APS has selected to resolve the in-vessel fuel effects utilizing WCAP-17788. Utilizing WCAP-17788 is expected to provide additional fiber margin above the current limit of 15 grams per fuel assembly.

GL 2004-02 notes that research and analysis efforts have suggested potential susceptibility of PWR recirculation sump screens to debris blockage during design basis accidents that require recirculation operation of the ECCS and CSS. The NRC requested that PWR licensees use NRC-approved methodology to evaluate the potential for adverse effects of post-accident debris blockage.

APS has completed the evaluation requested in accordance with the guidance of Nuclear Energy Institute (NEI) 04-07 [Ref. 4.30], the associated NRC Safety Evaluation (SE) [Ref. 4.28] and Section 3.2.1.2.3.3 of the Boiling Water Reactor Owners Group (BWROG) Utility Resolution Guide (URG) [13]. As a result, APS has modified the PVNGS units to greatly increase the effective surface area of the ECCS sump screens by removing the original screens and installing strainer modules above each sump. The surface area of the new sump screens was increased from 210 ft^2 to 3,142 ft^2 per sump. In addition, the design of the new strainers has been improved by adopting strainer geometry less susceptible to blockage. This increase in effective surface area and improved design assures that ECCS and CSS will perform their intended safety functions under any blockage conditions postulated to occur after a Loss of Coolant Accident (LOCA), including chemical effects. Other corrective actions included removal of Fiberfrax insulation in Containment and enhancements to PVNGS programs and procedures to improve control of transportable debris, thereby reducing potential blockage. Nukon insulation has been removed around the letdown delay coils.

To further reduce potential debris loading, the Microtherm (Units 1 and 2) and Min-K (Unit 3) insulation was removed from the reactor pressure vessel (RPV) head. This insulation removal was performed in conjunction with the reactor head replacement project for each unit. The new reactor heads are insulated with Transco RMI.

Physical modifications to Units 1 and 3 required by GL 2004-02 for the installation of larger ECCS sump strainers were completed by December 31, 2007, per the GL schedule. APS had requested and was granted an extension of the December 31, 2007, date for Unit 2 to install the larger sump strainers until the end of the spring 2008 refueling outage 2R14, based on late delivery of the strainer for installation in the fall 2006 Unit 2 Refueling Outage. The Unit 2 ECCS strainer installation was completed in 2R14 as scheduled. In addition, due to difficulties in completion of the confirmatory testing and analyses, an extension was granted to September 30, 2008. All confirmatory testing analyses were completed by September 30, 2008, as scheduled.

This addendum documents the completion of GL 2004-02 for PVNGS and compliance with NRC guidance as currently formulated for determining susceptibility of PWR recirculation sump screens to the adverse effects of debris blockage during design basis accidents that require recirculation operation of the ECCS and CSS.

APS used the NEI and NRC guidance, and the guidance in Section 3.2.1.2.3.3 of the BWROG URG [13] in the evaluation of the new containment sump strainers. The majority of the NEI and NRC guidance was used without deviations. However, a deviation was taken in the determination of the design basis strainer head loss. The design basis strainer head loss is based both on testing and analysis since the strainer testing performed did not include the total quantity of debris. The results of the evaluation described in Section 4 of this Addendum show that the Control Components, Inc. (CCI) pocket strainers experience a maximum head loss of 9.78 ft including chemical effects (Table 4-18). The resulting minimum ECCS/CSS pump NPSH and minimum strainer structural margin is 2.22 ft-water.

The performance testing used an initial flow rate of 11,600 gpm for the first hour of recirculation and 6,600 gpm for the remainder of the performance test. The initial flow of 11,600 gpm is based on ECCS and CS pumps at maximum flow. The 6,600 gpm is based on the CS and high pressure safety injection (HPSI) pumps operating at maximum flow for the duration of the test.

The impact of sump debris on the performance of the ECCS and CSS following a LOCA (downstream effects) at PVNGS was evaluated. The effects of debris ingested through the ECCS sump screen during the recirculation mode of the ECCS and CSS include erosive wear, abrasion, and potential blockage of flow paths. Erosive wear on components was determined to be insufficient to affect system performance. Similarly, the sump screen hole size precludes the blockage of the ECCS flow path.

The in-vessel downstream effects analysis for Palo Verde is consistent with the methodology from Revision 2 of WCAP-16793-NP and its associated Safety Evaluation. PVNGS meets the acceptance criteria for fuel cladding temperature (< 800°F), crud deposition thickness (< 50 mils), and grams of bypassed fiber per fuel assembly (< 15 g/assembly) set forth in WCAP-16793-NP and its associated Safety Evaluation utilizing the existing debris load and strainer testing. The calculated maximum temperature of the fuel cladding over the 30 days following the LOCA is less than 368.8 °F [14] and the calculated deposition thickness is 4.9 mils (125.7 microns) [14]. The fiber bypass debris amount is 13.8 grams per fuel assembly [11] [14].

Considering the overall parameters for debris generation, debris transport, chemical effects, downstream effects, in-vessel effects, testing methodology and strainer performance testing, and the resulting minimum (of NPSH and structural) margin of 2.22 ft-water, the objectives of GL 2004-02 are satisfied.

3.3 Revised Overall Compliance

The following overall compliance statement is an update to that which was provided in Revision 2 of the APS Supplemental Response to GL 2004-02[2].

This response summarizes the technical basis for the PVNGS ECCS strainer design and the associated programmatic controls that satisfy the commitments relative to GL 2004-02. The new sump strainer design complies with the revised NRC guidance for determining the susceptibility of PWR recirculation sump screens to the adverse effects of debris blockage during design basis accidents that require recirculation operation of the ECCS and CSS.

The ECCS sump strainers in PVNGS Units 1, 2, and 3 have been replaced under Design Master Work Order (DMWO) 2822654, per commitments to the NRC as documented in APS Letter 102-05336 dated September 1, 2005 [Ref. 4.90]. The Unit 1 sump strainer was replaced in the spring 2007 refueling outage; the Unit 3 sump strainer was replaced in the fall 2007 refueling outage; and the Unit 2 sump strainer was replaced in the spring 2008 refueling outage. The modifications were deemed necessary based on evaluations requested by GL 2004-02 which were performed in accordance with the guidance in NEI 04-07, *Pressurized Water Reactor Sump Performance Evaluation Methodology*, and the associated NRC SE [Ref. 4.28]. The assessment of impact of newly-discovered Microtherm and Temp-Mat insulation and Nukon insulation, that was not considered in chemical precipitate load definition, is performed in accordance with the guidance in NEI 04-07, and is augmented by (1) application of guidance in Section 3.2.1.2.3.3 *Method 3 – Break Specific Analysis using Break-Dependent Zone of Influence* of the BWROG URG [13] for computing ZOIs for restrained separation breaks, (2) using refined size distribution for destroyed Temp-Mat based on the results in Proprietary Alion Report ALION-REP-ALION-2806-01 [15], and using Temp-Mat erosion estimates based on Proprietary Alion Report ALION-REP-ALION-I006-04 [16].

The new sump strainers were procured from CCI, per PVNGS Specification 13-MN-1003 [Ref. 4.31]. The new design increased the screen size from approximately 210 ft^2 to 3,142 ft^2 per sump [Ref. 4.25]. This design provides sufficient area to ensure ECCS and CSS performance by accommodating any strainer blockage that is postulated to occur following a LOCA based on the results of the CCI strainer testing, strainer head loss analysis and comparative analysis documented in ALION-REP-APS-9199-02, *Technical Report: Assessment of Microtherm Insulation In the Palo Verde Reactor Cavities* [11]. The new strainer design includes sufficient margin for chemical effects. DMWO 2822654 also removed, from all three units, the Fiberfrax insulation from piping penetrations in the bioshield (steam generator [S/G] D-ring and pressurizer) walls, which reduced the amount of transportable debris in Containment. The Fiberfrax penetration seals were replaced with stainless steel sheet metal barriers to accomplish penetration isolation. Nukon insulation has been removed around letdown delay coils. In an effort to further reduce potential debris loading, the Microtherm (Units 1 and 2) and Min-K (Unit 3) insulation was removed from the reactor head in conjunction with the reactor head replacement project for each unit. The new reactor heads are insulated with Transco RMI.

[2] References cited in this Section using [Ref. X.Y] format refer to references provided in Revision 2 of APS Supplemental Response to GL 2004-02, not this Addendum. References cited using the format [X] are specific to this Addendum and are listed in the References Section.

New sump strainers are installed in the same location as the existing strainers and located on the containment floor directly over the sump pits. The new strainers supplied by CCI incorporate diverse geometry in the design, which is less susceptible to thin-bed effects than flat screens, and are constructed of perforated stainless steel plate. The new strainers are installed with approximately 3,142 ft^2 of strainer surface area per sump with holes having a nominal diameter of 0.083 inch. The new strainers are bolted with no gaskets or soft sealants and the screens are not welded. The combination of the CCI design, PVNGS large screen area, and limited fiber debris load results in open screen area and ample NPSH margin.

In each PVNGS unit, the suction supply for the ECCS and CSS pumps during recirculation following a LOCA is provided by two ECCS sumps, one for each safety-related train. The sumps are located on the lowest floor in Containment and are physically separated to preclude simultaneous damage to both screens.

The strainer head loss analysis is documented in N001-1106-00247 [Ref. 4.33] and ALION-REP-APS-9199-02 [11]. Calculation 13 MC SI-0250 [Ref. 4.32] verifies adequate available Net Positive Suction Head (NPSH) for the ECCS and CSS pumps based on the calculated head loss and resultant deaeration. The NPSH analysis utilizes the new head loss data for the replacement ECCS sump strainers based on the bounding headloss determined in ALION-REP-APS-9199-02 [11]. Study 13-MS-C043 determined the minimum ECCS strainer margin for GSI-191, which is the minimum of the hydraulic (NPSH) margin and structural margin. The results in 13-MS-C043 have been augmented by additional, new analysis that provides increased sump strainer structural capacity [17].

APS increased the refueling water tank (RWT) minimum water level to ensure adequate strainer submergence [Refs. 4.127 and 4.128].

Considering the overall parameters for debris generation, debris transport, chemical effects, downstream effects, in-vessel effects, testing methodology, strainer performance testing, increased structural capacity determination [18] and the resulting minimum (of NPSH and structural) margin of 2.22 ft, APS has demonstrated compliance with GL 2004-02.

The UFSAR will be updated with changes in accordance with 10 CFR 50.71(e), following adoption of WCAP-17788, as described in commitment 23, described in 3.4 of this Addendum.

3.4 Supplemental General Description and Schedule for Corrective Actions

The information provided in the *General Description of and Schedule for Corrective Actions* Section of Revision 2 of the APS Supplemental Response to GL 2004-02 continue to apply. The information below is supplemental to that which was provided in Revision 2. For each PVNGS Unit, a commitment is made to remove discrepant (i.e., not evaluated) fibrous insulation over the next two refueling outages for each Unit, beginning with the Fall 2016 Unit 3 refueling outage (3R19).

GL 2004-02 REGULATORY COMMITMENT	DUE DATE	REVISED DUE DATE OR STATUS
23. APS is participating in the PWROG program for establishing revised in-vessel debris limits. It is expected that a topical report (e.g., WCAP-17788) will be submitted for NRC review and approval after testing and analysis is completed. APS expects to resolve GSI-191 and GL 2004-02 for PVNGS after NRC issuance of the final safety evaluation for the topical report. APS will develop a plan for demonstrating compliance with the revised PWROG program limits and communicate that plan to the NRC within 60 days of the final NRC safety evaluation for the topical report (RCTSAI 4409509) (from Letter Number 102-06805, dated December 18, 2013).	60 days following issuance of final safety evaluation for WCAP-17788	Under NRC review
24. For PVNGS Unit 1 – Inspect a representative sample of RCS piping, including hot and cold legs, pressurizer surge and main spray lines and remove discrepant (i.e., not evaluated) fibrous insulation over the next two refueling outages	End of Unit 1R21 (Spring 2019) Target May 15, 2019	Some discrepant material removed in 1R19
25. For PVNGS Unit 2 - Inspect a representative sample of RCS piping, including hot and cold legs, pressurizer surge and main spray lines and remove discrepant (i.e., not evaluated) fibrous insulation over the next two refueling outages	End of Unit 2R21 (Fall 2018) Target December 1, 2018	Some discrepant material removed in 2R19
26. For PVNGS Unit 3 - Inspect a representative sample of RCS piping, including hot and cold legs, pressurizer surge and main spray lines and remove discrepant (i.e., not evaluated) fibrous insulation over the next two refueling outages, beginning with Fall 2016 Unit 3 refueling outage (3R19)	End of Unit 3R20 (Spring 2018) Target May 15, 2018	Some discrepant material removed in 3R19

3.5 Revised Strainer Structural Capacity Discussion

The following is an updated discussion of sump strainer structural capacity. The affected section is the response to item *k. Sump Structural Analysis*, of Revision 2 of the Supplementary response to Generic Letter 2004-02, page 3-141. Updates are indicated with margin bar.

1. Sump Strainer Structural Analysis

Provide the information requested in GL 2004-02 Requested Information Item 2(d)(vii).

GL 2004-02 Requested Information Item 2(d)(vii)

Verification that the strength of the trash racks is adequate to protect the debris screens from missiles and other large debris. The submittal should also provide verification that the trash racks and sump screens are capable of withstanding the loads imposed by expanding jets, missiles, the accumulation of debris, and pressure differentials caused by post-LOCA blockage under flow conditions.

Summarize the design inputs, design codes, loads, and load combinations utilized for the sump strainer structural analysis.

The strainers are installed in locations that are remote to high-energy line breaks and are located outside of the bio-shield wall. The strainers consist of pocket cartridges, which are assembled together into strainer modules. These modules are tied together using a module support structure and are supported at the base by a sub-floor that covers and seals the entire sump. The sub-floor is attached to the base of the columns of a modified version of the previous sump screen frame.

CCI analyzed the imposed stresses on the ECCS sump strainer standard pocket cartridge [Ref. 4.22], the strainer module and support structure [Ref. 4.24], and the supporting sub-floor [Ref. 4.23]. Also these components were further assessed for a larger differential pressure by CCI [Ref. 4.67].

In the strainer component and supporting structure final stress evaluation, the limits of the ASME B&PV Code, Subsection NF, *Supports*, are satisfied for the original loading conditions. The requirements of the American Institute of Steel Construction (AISC) Manual of Steel Construction were also considered for the perforated plates used in the strainer.

As the strainer is not a pressure-retaining part, it is not subjected to any pressure transients or hydrostatic pressure during normal operation of the unit. As shown through testing, with the strainer areas covered with debris and the pumps in operation, there will still be some flow through the strainer. Hence, the critical components with respect to loads caused by the pressure drop are the plates and perforated plates that are part of the strainer modules.

The strainer components and supporting structures were evaluated for the load combinations in the PVNGS UFSAR. The analysis determined that the governing load combination was $1.7\ S > D + P + Ta + E'$ where S is the AISC normal allowable stress, D

is dead load, P is the stresses caused by differential pressure across the strainer during flooded condition, E' is SSE earthquake-induced stresses, and Ta is accident thermal stresses. As the LOCA condition governs, the earthquake-induced stresses include the effects of sloshing and consideration of the hydrodynamic masses. The amounts of debris considered for the calculation of the equivalent pressure which acts over the two strainer modules (large and small modules) were 520 lbs and 325 lbs, which corresponds to 32.5 lbs/cartridge since there are 16 or 10 cartridges in the two strainer modules.

The cartridge analysis was performed using ANSYS, version 10.0. Stresses were calculated for both the perforated and unperforated plates. For the AISC evaluation, an allowable stress increase factor of 1.7 for SSE was used in accordance with the load combinations. For the ASME evaluation, an allowable stress increase factor of 1.5 was used. For both the perforated and unperforated plates, the maximum membrane stress, σ_m, was calculated to be less than 1.7 times 0.6 times the yield stress (AISC) and less than 1.5 times the calculated allowable stress (ASME). The maximum membrane stress plus bearing stress, $\sigma_m + \sigma_b$, was calculated to be is less than 1.7 times 0.66 times the yield stress (AISC) and less than 1.5 times the calculated allowable stress (ASME). Thus, all stresses are below the stress limits for load combinations for SSE accelerations.

The analysis of the modules was also performed using ANSYS, Version 10.0. Since standard modules consist of the support, the duct, and either 10 or 16 cartridges, a module with 16 cartridges is conservatively considered in the analysis. The maximum membrane stress, σ_m, was calculated to be less than 1.7 times 0.6 times the yield stress (AISC) and less than 1.5 times the calculated allowable stress (ASME). The maximum membrane plus bearing stress, $\sigma_m + \sigma_b$, was calculated to be less than 1.7 times 0.66 times the yield stress (AISC) and less than 1.5 times the calculated allowable stress (ASME). Thus, all stresses are below the stress limits for load combinations for SSE accelerations.

For the various component parts of the strainer module, e.g., duct lower plate, duct upper plate, duct side panel, etc., the maximum membrane stress, σ_m, was calculated to be less than the material yield strength. Further, the maximum membrane plus bending stress, $\sigma_m + \sigma_b$, was calculated to be less than the cumulative maximum stress plus bending stress.

In the sub-floor calculation, AISC Manual of Steel Construction, 9th Edition limits are satisfied. The strainer modules are included with a beam and spring model representing its real center of gravity, mass, and stiffness. The springs were defined so that the beam model and the structural model have the same fundamental natural frequencies in all coordinate planes.

The ANSYS computer program was used to calculate the plate stress at the strainer opening. The maximum membrane plus bending stress was calculated to be less than the allowable membrane stress limit. The computer program also calculated the bending stresses for quadratic and rectangular plate geometries. The maximum bending stresses were below the allowable stress limit. Also, the maximum bending stresses for the sump access base plate and access cover are also calculated to be below the allowable stress limit.

The CCI calculation 3SA-096.043 [Ref. 4.67] structurally evaluates the maximum allowable stress difference for the three major strainer components consisting of the cartridge, module, and sub-floor. The CCI calculation uses the same geometry and calculation models to find the maximum allowable pressure difference. Using the AISC limits, the calculations [Refs. 4.22, 4.23, and 4.24] show the maximum allowable pressure difference (at 70 °F) over each of these three major strainer components as follows:

- Cartridge: 6.527 psi (0.045 MPa, 15 ft WC)
- Module: 4.496 psi (0.031 MPa, 10.4 ft WC)
- Sub-floor: 6.527 psi (0.045 MPa, 15 ft WC)

The weakest component, which is also the limiting condition, was found to be the module (frame structure).

Maximum Allowable Pressure Difference

The original analyses performed [Refs. 4.22, 4.23, and 4.24] were based on a pressure difference of 5.0 ft. WC. An additional analysis [Ref. 4.67] was performed to determine the maximum allowable pressure difference. The maximum allowable pressure difference for the strainer structure and the sub-floor was determined to be 10.4 ft. WC at the material temperature of 70°F [Ref. 4.44].

Appendix A of [Ref. 4.67] shows, that the strainer assembly is capable of bearing a differential pressure of ΔP = 12 ft. WC at a temperature of 170°F, if ASME limits are used for the plate and shell type parts of the frame support. The stresses in the sub-floor structure consisting mainly of a beam type design are still below the AISC limits for the target loading (12 ft. WC 70°F).

The maximum allowable pressure difference is therefore 12 ft. WC at 170°F for all three major strainer components.

4 Qualification by Analysis

This Section describes the approach, inputs and analyses that form the basis for the conclusion that the configuration that exists after all remedial actions are completed will satisfy the objectives of GL 2004-02.

4.1 Analytical Qualification Approach

The overall analytical qualification approach is based on comparative analysis with results of existing analyses and testing, both by APS and other plants with CCI ECCS sump strainers. The comparative analysis demonstrates that the original acceptance criteria remain satisfied in the presence of the newly-discovered insulation that will not be removed (see Table 3-1).

4.2 Key Inputs

This Sub-section describes the inputs, (i.e., previous analyses, results of testing by other plants with CCI strainers and industry documents), that are used to implement the analytical qualification approach for demonstrating compliance with the objectives of GL 2004-02.

4.2.1 APS Analyses of Record

As previous APS analyses of record were prepared under applicable quality programs, design inputs (other than newly-discovered insulation), methods and results in previous APS analyses of record are legitimate inputs for use in the analytical qualification of newly-discovered insulation that will not be removed. Applicable previous analyses of record include:

- N001-1106-00002, *Debris Generation Due to LOCA within Containment for Resolution of GSI-191* [19].
- N001-1106-00003, *Post-LOCA Debris Transport for Resolution of GSI-191,* Calculation Number 2005-09080 [20].
- N001-1106-00231, WCAP-16530,*Post-LOCA Chemical Effects Analysis in Support of GSI-191* [21].
- N001-1106-00229, Chem Effects Test (Spec), *Chemical Effect Head Loss Test Specification* (R2) [22].
- N001-1106-00227, Chem Effects Test (Report), *Chemical Effects Test* [23].
- N001-1106-00247, Determination of Head Loss Bump-Up Factor For ECCS Strainers [24].

The analyses of record cited above represent the configuration that existed before the newly-discovered insulation that is addressed in this assessment were identified.

Prior to the configurations addressed in the above-cited analyses of record, there was an earlier configuration of insulation at Palo Verde, which was addressed in earlier versions of analyses. Among these is N001-1106-00003, *Post-LOCA Debris Transport for Resolution of GSI-191,* Calculation Number 2005-09080 [25], from which information was used in this assessment.

4.2.2 Strainer Structural and Hydraulic Capacity

The original structural capacity of the strainers over the temperature range of 77 °F to 252 °F is documented in N001-1106-00228 [26]. The revised structural capacity of the strainers over the temperature range of 77 °F to 170 °F is documented in N001-1106-00176 [17]. The structural capacity of the strainers over the temperature range of 176 °F to 252 °F remains defined in N001-1106-00228 [26].

The hydraulic limit of the strainers over the temperature range of 77 °F to 252 °F is defined by NPSH margin in Summary of CCI Strainer Head Loss Testing [27].

Table 4-1 summarizes the current temperature-dependent structural and hydraulic capacity of the strainers. The overall strainer limit at each temperature is the governing limit based on revised structural and existing NPSH limits.

Table 4-1: Strainer Structural and Hydraulic Capacity

Temp [5] (°F)	Original Structural Limit [1] (ft-Water)	Revised Structural Limit (ft-Water)	Minimum Hydraulic Limit [3] (ft-Water)	Overall Strainer Limit (ft-Water)
77	10.40	12.00 [2]	27.25	12.00 [2]
86	10.40	12.00 [2]	27.30	12.00 [2]
104	10.32	12.00 [2]	27.09	12.00 [2]
122	9.98	12.00 [2]	26.16	12.00 [2]
140	9.74	12.00 [2]	23.90	12.00 [2]
158	9.48	12.00 [2]	20.35	12.00 [2]
160	9.45 [4]	12.00 [2]	19.77 [4]	12.00 [2]
170	9.31 [4]	12.00 [2]	16.88 [4]	12.00 [2]
174.9	9.25 [4]	9.25 [1, 4]	15.47	9.25 [1, 4]
175	9.25 [4]	9.25 [1, 4]	15.42	9.25 [1, 4]
176	9.23	9.23 [1]	15.03 [4]	9.23 [1]
179.78	9.18 [4]	9.18 [1, 4]	13.71 [4]	9.18 [1, 4]
180	9.17 [4]	9.17 [1, 4]	13.63	9.17 [1, 4]
193.8	8.98	8.98 [1]	7.71	7.71
252	8.39	8.39 [1]	7.93	7.93

Notes:

1. N001-1106-00228 [26]
2. N001-1106-00176 [17]
3. Summary of CCI Strainer Head Loss Testing [27]
4. Value is based on linear interpolation between published values
5. Temperature value decimal places are intentionally different, designed to be exactly the same as used in associated reference documents

4.2.3 Results of Headloss Testing by Other Plants with CCI Strainers

Whereas APS headloss testing did not include microporous insulation debris, to enable comparative quantification of APS headloss in the presence of Microtherm, results of testing performed by Salem Unit 2 are used [28]. Details are discussed later in Section 4.7.2 of this document.

4.2.4 Industry Documents

In addition to plant-specific documents, information contained in industry guidance and technical documents are used, including:

- NEI 04-07, Volume 2 – *Safety Evaluation by the Office of Nuclear Reactor Regulation Related to NRC Generic Letter 2004-02*, Revision 0, December 6, 2004, (NEI 04-07 SER) [29].
- NEDO-32686-A, *Utility Resolution Guidance for ECCS Suction Strainer Blockage*, BWROG [13].
- NUREG/CR-6808 (LA-UR-03-0880) *Knowledge Base for the Effect of Debris on Pressurized Water Reactor Emergency Core Cooling Sump Performance*, February 2003 [30].
- NUREG/CR-6772, *GSI-191: Separate-Effects Characterization of Debris Transport in Water* [31].
- ANSI/ANS-58.2-1988, *Design Basis for Protection of Light Water Nuclear Power Plants Against the Effects of Postulated Pipe Rupture*, October 6, 1988 [32].

4.3 Acceptance Criteria

Five acceptance criteria are considered in qualification of the conditions that exist in the presence of newly-discovered insulation that will not be removed.

The acceptance criteria are:

(1) strainer headloss less than available NPSH margin,

(2) differential pressure across the strainer less than strainer structural capacity, and

(3) downstream effects, including:

   a. in-vessel fiber load less than 15 grams per fuel assembly, and

   b. equipment particulate wear quantities less than the allowables determined in previous analyses in N001-1106-00225 [33], N001-1106-00012 [34], N001-1106-00011 [35] and N001-1106-00013 [36],

(4) Fuel Cladding Temperature less than 800 °F,

(5) Crud deposition thickness less than 50 mils.

4.4 Debris Generation

The debris generation Analysis of Record determined that Break S1, at the Hot Leg (HL) of the Loop 2 Steam Generator, was the limiting break. Break S1 and other breaks considered in the debris generation Analysis of Record are shown in Figure 4-1 (excerpted from Figure 3-1 Break Locations in Revision 2 of APS Supplemental Response to GL 2004-02 [10]).

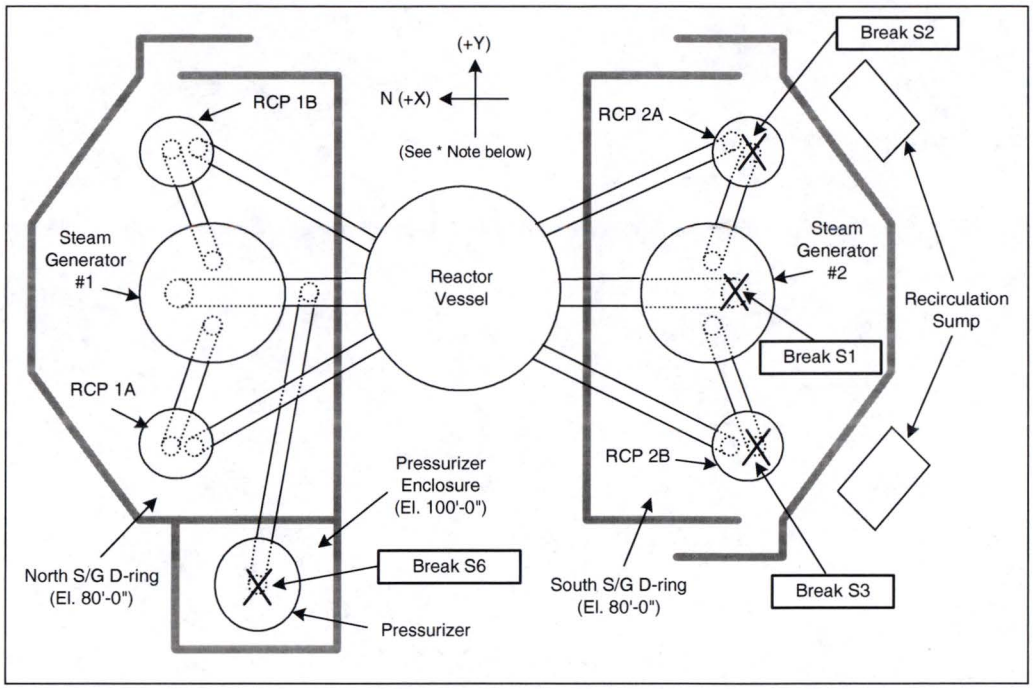

Figure 4-1: Break Locations in Revision 2 of the APS Supplemental Response to GL 2004-02

The debris generation Analysis of Record did not explicitly consider breaks at RPV nozzles as it was incorrectly assumed that the RPV and piping insulation was RMI. The break locations considered in this qualification analysis are shown in Figure 4-2.

Figure 4-2: Break Locations Considered in the Updated Qualification Analysis

Addendum to Supplemental Response to NRC Generic Letter (GL) 2004-02, Revision 2

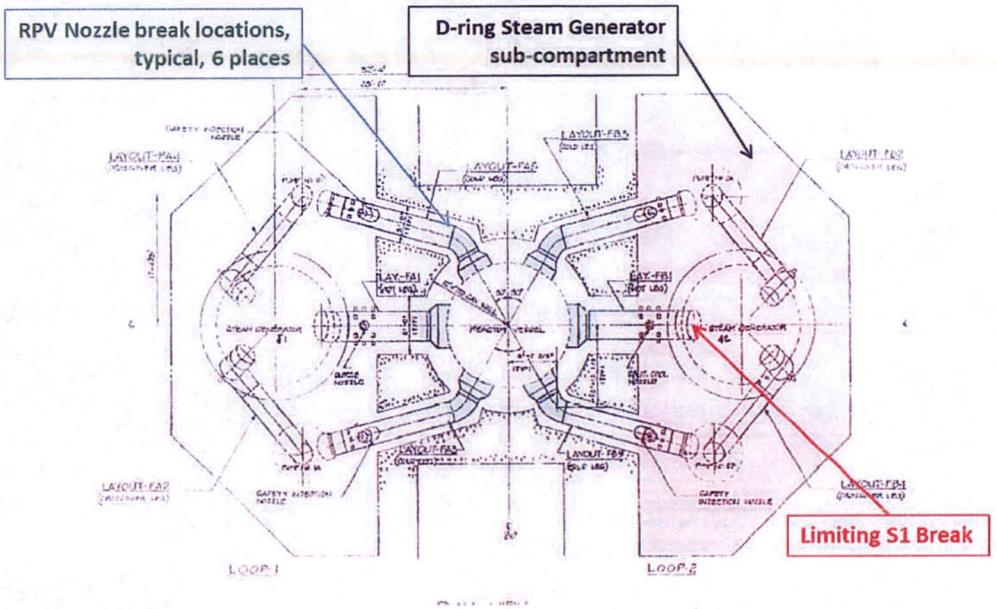

4.4.1 Zone of Influence

Zone of Influence (ZOI) values for insulation and coatings reported in Revision 2 of the APS Supplemental Response to GL 2004-02 [10] are summarized in Table 4-2 (Table 4-2 is an excerpt of Table 3-3: *PVNGS Zone of Influence,* from Revision 2 of the APS Supplemental Response to GL 2004-02). The ZOIs in Table 4-2 are for unrestrained double-ended guillotine pipe breaks.

Table 4-2: Zone of Influence Values for Insulation and Coatings

Insulation/Coating	ZOI Radius/ Break Diameter (r/D)
Piping (Transco RMI or Mirror RMI)	28.6
Equipment RMI (Transco RMI)	2.0
Nukon (All)	17.0
Temp-Mat (All)	11.7
Thermo-Lag	28.6 (1)
Alpha Cloth	28.6 (1)
Qualified Coatings - Epoxy	4.0
Qualified Coatings – Inorganic Zinc (IOZ)	10.0
Unqualified Coatings and Degraded Qualified Coatings	All assumed to fail

(1) There is no information in the NEI or NRC documents [Refs. 4.28 and 4.30] regarding the ZOI for Thermo-Lag 330 or Alpha Cloth. Analysis assumed that the ZOI for this material was equal to the largest ZOI recommended by the NEI and NRC guidance documents (28.6 r/D). This is conservative and requires no further justification.

4.4.1.1 Unrestrained Break Microtherm ZOI

At the time Revision 2 of the APS Supplemental Response to GL 2004-02 was issued, it was considered that all Microtherm at APS had been removed. This is why Table 4-1 (and Revision 2 of the APS Supplemental Response to GL 2004-02) did not discuss a ZOI for Microtherm.

Microtherm at APS is encapsulated in 24 gage stainless steel cassettes whose construction is equal to or more robust than Transco RMI panels for which ZOI testing was reported in the BWR Owner's Group Utility Resolution Guide (BWR-URG), NEDO-32686-A [13]. The robustness, and, therefore, the destruction pressure of encapsulated Microtherm insulation is initially a function of the strength and resistance to destruction of the encapsulation, (i.e., cassettes); not the Microtherm that is contained in the cassettes. Therefore, if the Microtherm insulation encapsulation is not destroyed, the Microtherm contained inside the encapsulation is likewise not destroyed.

Encapsulated Microtherm insulation at PVNGS consists of stitched or quilted panels, which are better suited for encapsulation in a cylindrical insulation application [37]. Stitching in overstitched and quilted Microtherm panels essentially creates individual "pockets" of microporous material [37]. Microporous material does not "move" from one pocket to another; (i.e., each pocket maintains its constituent material even when flexed) [37]. Based on this, it is unlikely that all Microtherm powder within a damaged encapsulation cassette would be damaged and escape if the cassette is damaged. Nonetheless, to ensure a conservative approximation, it is assumed that all Microtherm within an encapsulation cassette that is totally or partially within its ZOI is completely destroyed and can escape into surrounding water.

The URG [13] determined the destruction pressure of the RMI cassettes that were tested to be 190 psig. Subsequently, to account for unknowns and ensure conservative usage, the destruction pressure of the RMI cassettes was reduced (by 40%) to 114 psig in NEI 04-07, *Volume 2 – Safety Evaluation* [29].

The ZOI given in Table 3-2, *Revised Damage Pressures and Corresponding Volume-Equivalent Spherical ZOI Radii*, of NEI 04-07, Volume 2 – Safety Evaluation [29] for Transco RMI and Darchem Darmet is 2.00D. On the basis of the above discussion, the ZOI of Microtherm insulation encapsulation cassettes is taken as 2.00D, corresponding to a destruction pressure of 114 psig. The 2.00D ZOI is applicable for unrestrained break situations. For situations where the axial and/or radial separation at the break is restrained, an alternate method of computing ZOI, based on the destruction pressure, is applied.

4.4.1.2 Restrained Break ZOI

Potential pipe breaks at RPV nozzles will be partially restrained in that the amount of radial motion of the broken pipe will be limited by the concrete penetration through which the pipe passes, and axial motion of the broken pipe will be limited by the restraint effect of Steam Generator supports (for Hot Leg breaks) and Reactor Coolant Pump supports (for Cold Leg breaks). The restrained separation between the ruptured pipe and RPV, as well as the location of the break (within the region between the RPV and the concrete biological shield wall that surrounds the RPV), affects the ZOI associated with pipe breaks at RPV nozzles.

Of the three types of breaks illustrated in Figure 7-2, *Fluid Jet Models*, of ANSI/ANS-58.2-1988 [32], model (B), *Jet From Circumferential Break with Ends Restrained*, is the most conservative to use because, due to its 360-degree cylindrical shape, it will result in more destruction of

encapsulated Microtherm and Temp-Mat on the RPV than model (A), *Jet From Circumferential Break with Unrestrained Ends*, or model (C), *Jet From Longitudinal Break*. If using model (A), *Jet From Circumferential Break with Unrestrained Ends*, it would be appropriate to consider part of the jet being directed out through the penetration at the break; using model (B) does not include this consideration. If using model (C), *Jet From Longitudinal Break*, a limited, uni-directional "cone" shape would need to be considered, which would affect a smaller portion of encapsulated Microtherm than model (B), and would result in little or no destruction of Temp-Mat.

The methodology employed for computing the ZOIs for encapsulated Microtherm and Temp-Mat for breaks at RPV nozzles is taken directly from Section 3.2.1.2.3.3 *Method 3 – Break Specific Analysis using Break-Dependent Zone of Influence,* of the BWROG URG [13].

Restrained break ZOIs were developed computed as:

$$ZOI_{calc} = (ZOI_{rest} / ZOI_{unrest}) \times SF \times ZOI_{nom}, \text{ where}$$

ZOI_{calc} is the ZOI used in debris generation calculations
ZOI_{rest} is the ZOI for a restrained break using BWROG URG Section 3.2.1.2.3.3 "Method 3"
ZOI_{unrest} is the ZOI for an unrestrained break using BWROG URG Section 3.2.1.2.3.3 "Method 3"
SF is a (voluntary) safety factor (2.0) to add conservatism
ZOI_{nom} is the "nominal" ZOI based on industry guidance documents such as NEI 04-07, *Volume 2 – Safety Evaluation* [29], applicable for unrestrained breaks

A summary of the ZOIs used to compute debris generation resulting from RPV nozzle breaks is provided in Table 4-3.

Table 4-3: ZOIs Used in Debris Generation Calculations

Item	Microtherm	Temp-Mat	Description
ZOI_{nom}	2.00D	11.70D	Applicable to D-ring break cases
ZOI_{calc} CL Break	1.54D	9.00D	Used for RPV nozzle break cases
ZOI_{calc} HL Break	1.32D	8.42D	Used for RPV nozzle break cases
ZOI_{calc} CL Break	n/a	2.86D	Used for RPV nozzle break cases to define sub-region of total ZOI for refined (fines/small) size distribution
ZOI_{calc} HL Break	n/a	2.45D	

For debris generation calculations for RPV nozzle breaks, the spherical volume of the ZOI is conformed to an equivalent volume having the "pancake-saddle" shape of the region between the RPV and the concrete biological shield wall that surrounds the RPV. The conformance of the volume into the "pancake-saddle" shape results in a greater reach of the ZOI and hence a larger quantity of insulation is affected than if the ZOI was considered to be spherical.

4.4.2 Size Distribution

4.4.2.1 Microtherm

All destroyed Microtherm is considered to be fines.

4.4.2.2 Temp-Mat

Since all newly-discovered Temp-Mat in the D-ring Steam Generator Sub-compartments will be or has been removed, no newly-discovered Temp-Mat is destroyed due to breaks in the D-rings.

The size distribution of Temp-Mat destroyed by breaks at RPV nozzles is based on results in proprietary document ALION-REP-ALION-2806-01 [15]. The size distribution for Temp-Mat in ALION-REP-ALION-2806-01 is based on two sub-regions of the overall ZOI, 3.7D ZOI and 3.7D-11.7D ZOI.

4.4.3 Temp-Mat Density

Revision 2 of N001-1106-00003 [25], which is an earlier version of the *Debris Transport Calculation* [20], notes that the density of Temp-Mat is 11.8 lb/ft^3. The density of Nukon is 2.4 lb/ft^3. Hence, Temp-Mat is approximately 5 times as dense as Nukon (11.8 lb/ft^3 vs 2.4 lb/ft^3). When estimating total mass of generated or transported fiber, this difference in density is taken into account.

4.4.4 Flow Conditions

As discussed in Revision 2 of the APS Supplemental Response to GL 2004-02 item 3.g.1, the maximum ECCS (recirculation) sump flow rate is 11,600 gpm (per sump) and is based on HPSI, low pressure safety injection (LPSI), and containment spray system (CSS) pumps operating at pump maximum flow. The maximum flows for the HPSI, LPSI, and CSS pumps are 1,400 gpm, 5,000 gpm, and 5,200 gpm respectively. LPSI pumps receive an automatic signal to trip upon initiation of the recirculation actuation signal (RAS). Expected post-LOCA flow to each sump is therefore 6,600 gpm. There are two independent trains of HPSI, LPSI, and CSS.

There are two single-active failures that pertain to ECCS sump flow. They are (1) failure of an ECCS train to actuate at the Safety Injection Actuation Signal (SIAS), and (2) failure of an LPSI pump to trip at the RAS.

4.4.4.1 Failure of an ECCS Train to Actuate at SIAS

For this scenario, one ECCS train operates during injection (one HPSI, LPSI, and CS pump) and recirculation (one HPSI and CS pump). After the RAS, all flow (one HPSI and CS pump) is to one sump strainer with 100% of the postulated post-LOCA debris. In terms of expected debris transport per operational strainer, this condition is similar to Flow Scenarios S1, S2 and S3 in N001-1106-00003 [20].

4.4.4.2 Failure of a LPSI Pump to Trip at RAS

For this scenario, both ECCS trains operate during injection and recirculation. In the faulted train (train where LPSI fails to trip), the recirculation flow to the strainer is from one HPSI, CS, and LPSI pump. For the non-faulted train, (i.e., train where LPSI trips as designed), the flow is from

one HPSI and CS pump. In terms of expected debris transport per operational strainer, this condition is similar to Flow Scenario S5 in N001-1106-00003 [20] except that the failure to trip LPSI is considered in one train only.

Three conditions are possible outcomes for the failure of a LPSI pump to trip at RAS. They are (1) LPSI pump is secured shortly after RAS, as directed by emergency operating procedures, (2) LPSI pump is secured at some point in the mission time, and (3) LPSI pump remains on throughout the mission time.

Flow Condition Case 1: If the LPSI pump is secured shortly after RAS, the normal desired condition is restored, equal (6,600 gpm) flow occurs in both trains and each train attracts approximately 50% of transported debris. From a sump strainer maximum headloss standpoint, this condition is bounded by the Failure of an ECCS Train to Actuate at SIAS condition discussed in Section 4.4.4.1.

Flow Condition Case 2: If the LPSI pump is secured at some point in the 30-day mission time, the normal desired condition is restored, equal (6,600 gpm) flow occurs in both trains but between 50%-70% debris accumulation occurs at the faulted (and recovered) train strainer, and 30%-50% debris accumulation occurs in the normally–operating train. From a sump strainer maximum headloss standpoint, this condition is bounded by the Failure of an ECCS Train to Actuate at SIAS condition discussed in Section 4.4.4.1.

Flow Condition Case 3: If the LPSI pump remains on throughout the 30-day mission time, approximately 70% debris accumulation occurs at the faulted (11,600 gpm) train strainer, and approximately 30% debris accumulation occurs in the normally–operating train (6,600 gpm). If the faulted train in Case 3 experiences headlosses within NPSH and structural limits, there is no adverse condition. If the faulted train in Case 3 becomes inoperable, the condition reverts to that of single train operation, discussed in Section 4.4.4.1, Failure of an ECCS Train to Actuate at SIAS, except that 30%-50% accumulation of debris will occur at the single operating strainer. In effect, the failed train strainer will have acted as a sacrificial debris accumulator. Consequently, from a sump strainer maximum headloss standpoint, this condition is bounded by the Failure of an ECCS Train to Actuate at SIAS condition discussed in Section 4.4.4.1.

4.4.5 Debris Generation Analysis Cases

Three debris generation location cases are considered in assessment of newly-discovered insulation. These location cases are:

Break Case 1: Hot Leg break at Loop 2 Steam Generator (the original, S1, bounding break location)

Break Case 2: Cold Leg RPV Nozzle break (new)

Break Case 3: Hot Leg RPV Nozzle break (new)

For each of the three break location cases above, three flow scenarios are considered. These are:

- Flow Scenario 5 at which LPSI is not secured after RAS (resulting in 70% of total recirculation flow), discussed in Section 4.4.4.2

- Flow Scenario 5 at which LPSI is secured after RAS (resulting in 30% of total recirculation flow), discussed in Section 4.4.4.2

- Flow Scenarios S1, S2 and S3, discussed in 4.4.4.1

A complete description of a debris generation and debris transport analysis case is achieved by a combination of the above location cases and flow scenario case descriptions.

Table 4-4 summarizes the debris generation and debris transport analysis cases, and their associated recirculation flow, that are considered in assessment of the insulation in Table 3-1, that are resolved by analytical acceptance.

Table 4-4: Debris Generation and Debris Transport Analysis Cases

Break Case ID	Break Location	Flow Scenario	Flow (gpm)
1	S1 (SG2@HL)	5 LPSI on	16,600
1	S1 (SG2@HL)	5 LPSI off	6,600
1	S1 (SG2@HL)	1, 2, 3	6,600
2	RPV CL 2A	5 LPSI on	16,600
2	RPV CL 2A	5 LPSI off	6,600
2	RPV CL 2A	1, 2, 3	6,600
3	RPV HL 2	5 LPSI on	16,600
3	RPV HL 2	5 LPSI off	6,600
3	RPV HL 2	1, 2, 3	6,600

4.4.5.1 Hot Leg Break at Loop 2 Steam Generator

Debris generation analysis of a break at the Loop 2 Steam Generator (Break Case 1) is based on the following:

- Considers removal of Temp-Mat on cross-over piping and at resistance-temperature detectors (RTDs) on Cold Legs in both Loops.
- Considers no jet impinges on RPV through D-ring wall opening on Microtherm band around RPV based on being outside the 2.00D ZOI.
- Considers no jet impingement on Temp-Mat on the RPV at the Microtherm to RMI transition based on robust barrier.
- Considers no debris is generated in Loop-1 based on robust barrier.
- For chemical effects,
    - considers that the Reactor Cavity will flood and flow to the D-ring via 4-inch diameter pipe 051-XCDA
    - considers removal of Nukon insulation (see Table 3-1).

4.4.5.2 RPV Nozzle Breaks

Debris generation analysis of breaks at RPV nozzles (Break Cases 2 and 3) is based on the following:

- Considers blowdown to D-rings and Reactor Cavity based on flow area ratios.
- Considers Microtherm destruction based on restrained separation of ruptured pipe and RPV nozzle.
- Considers limited transport of Temp-Mat from the Reactor Cavity based on refined size distribution and computational fluid dynamics (CFD)-based turbulent kinetic energy (TKE) estimates that show that only Fines Temp-Mat is able to transport.
- Considers all Temp-Mat at RPV Cold Leg (CL) discharge elbows is removed, (see Table 3-1).
- Assumes Temp-Mat on affected CL at RTDs has been removed, (see Table 3-1).
- For chemical effects,
  - considers that the Reactor Cavity will flood and flow to the D-ring via Vaneaxial fan ducts and 051-XCDA-4,
  - considers removal of Nukon insulation (see Table 3-1).

4.4.5.3 Debris Generation Results

Table 4-5: Temp-Mat and Microtherm Debris Generation Results

Break Case[1]	Break Location[1]	Flow Scenario[1]	Generated to Cavity Temp-Mat Fines (ft^3)	Generated to Cavity Temp-Mat Small/Large (ft^3)	Generated to Cavity Microtherm Particulate (ft^3)	Generated to D-ring Temp-Mat Small/Fine (ft^3)	Generated to D-ring Temp-Mat Large (ft^3)	Generated to D-ring Microtherm Particulate (ft^3)
1	S1 (SG@HL)	5 LPSI on	0.0	0.0	0.0	0.0	0.0	0.0
1	S1 (SG@HL)	5 LPSI off	0.0	0.0	0.0	0.0	0.0	0.0
1	S1 (SG@HL)	1, 2, 3	0.0	0.0	0.0	0.0	0.0	0.0
2	RPV CL 2A	5 LPSI on	1.7	8.5	9.0	0.7	0.5	6.3
2	RPV CL 2A	5 LPSI off	1.7	8.5	9.0	0.7	0.5	6.3
2	RPV CL 2A	1, 2, 3	1.7	8.5	9.0	0.7	0.5	6.3
3	RPV HL 2	5 LPSI on	1.8	8.4	9.9	0.7	0.5	6.9
3	RPV HL 2	5 LPSI off	1.8	8.4	9.9	0.7	0.5	6.9
3	RPV HL 2	1, 2, 3	1.8	8.4	9.9	0.7	0.5	6.9

1. See break location and flow descriptions in Section 4.4.5

4.5 Debris Transport

4.5.1 D-ring Steam Generator Sub-compartment Breaks

4.5.1.1 Flowpath

Flowpaths to ECCS Sump Strainers for debris that is destroyed in, or transports into, the D-ring Steam Generator sub-compartments are discussed in N001-1106-00003 [20].

4.5.1.2 Fibrous Debris Transport Fractions

The maximum transport fraction associated with Nukon in N001-1106-00003 are shown in Table 4-6, (which is Table 5.1-1 of N001-1106-00003 [20]). Transport fractions associated with Nukon are used for Temp-Mat that is destroyed in, or transports into, D-ring Steam Generator sub-compartments after destruction. The size distribution used in N001-1106-00003 [20] combines Fines and Small Pieces into a single category.

Table 4-6: D-ring Break Transport Fractions

Table 5.1-1: Debris Transport Fractions & Fractions of Debris Transported to the Sump

Debris Type	Size Distribution Fraction	Debris Transport Fraction (Scenario/Break)				Fraction of Debris at Sump Screen (Scenario/Break)			
		1/S2	2/S2	3/S3	5/S2	1/S2	2/S2	3/S3	5/S2
Mirror RMI									
Fines	0.05	1.00	1.00	1.00	1.00	0.05	0.05	0.05	0.05
Small Pieces / Large Pieces	0.95	0.00	0.00	0.00	0.00	0.00	0.00	0.00	0.00
Sum	**1.0**	-	-	-	-	**0.05**	**0.05**	**0.05**	**0.05**
Transco RMI									
Fines	0.05	1.00	1.00	1.00	1.00	0.05	0.05	0.05	0.05
Small Pieces / Large Pieces	0.95	0.00	0.00	0.00	0.00	0.00	0.00	0.00	0.00
Sum	**1.0**	-	-	-	-	**0.05**	**0.05**	**0.05**	**0.05**
Nukon									
Fines/ Small Pieces	0.60	1.00	1.00	1.00	1.00	0.60	0.60	0.60	0.60
Large Pieces	0.40	0.00	0.00	0.00	1.00	0.00	0.00	0.00	0.40
Sum	**1.0**	-	-	-	-	**0.60**	**0.60**	**0.60**	**1.00**
Coatings									
Fines	-	1.00	1.00	1.00	1.00	1.00	1.00	1.00	1.00
Chips	-	0.00	0.00	0.00	0.00	0.00	0.00	0.00	0.00
Foreign Materials									
Labels/ Glass Lighting	-	0.00	0.00	0.00	0.00	0.00	0.00	0.00	0.00

4.5.1.3 Particulate Debris Transport Fractions

The transport fraction for all particulate debris, including Microtherm, is 1.0, (i.e., 100% transport).

4.5.2 Reactor Pressure Vessel Nozzle Breaks

4.5.2.1 Flowpaths

Debris that is destroyed from breaks at the Hot Leg or Cold Leg nozzles at the RPV can blowdown to:

i. the Refueling Cavity via six 16 inch by 22 inch openings in the permanent reactor cavity refueling pool seals [38],
ii. the D-ring Steam Generator sub-compartments via the Hot Leg and Cold Leg piping penetrations through the concrete (biological shield wall) D-ring structure, and
iii. the Reactor Cavity, via the space between the RPV and concrete biological shield wall that surrounds the RPV.

The Refueling Cavity and piping penetrations through the concrete (biological shield wall) D-ring structure have direct access to the D-ring Steam Generator sub-compartments. Consequently, any destroyed insulation that transports to either the Refueling Cavity or through the piping penetrations through the concrete (biological shield wall) D-ring structure will be subject to transport from the D-ring Steam Generator sub-compartments to the sump strainer (as discussed in Section 4.5.1).

The flowpath from the Reactor Cavity to the D-ring Steam Generator sub-compartments, and on to the sump strainers, is via four air circulation ducts which run from elevation 69 ft in the Reactor Cavity to vane-axial fans at elevation 87 ft. This flowpath is illustrated in Figure 4-3.

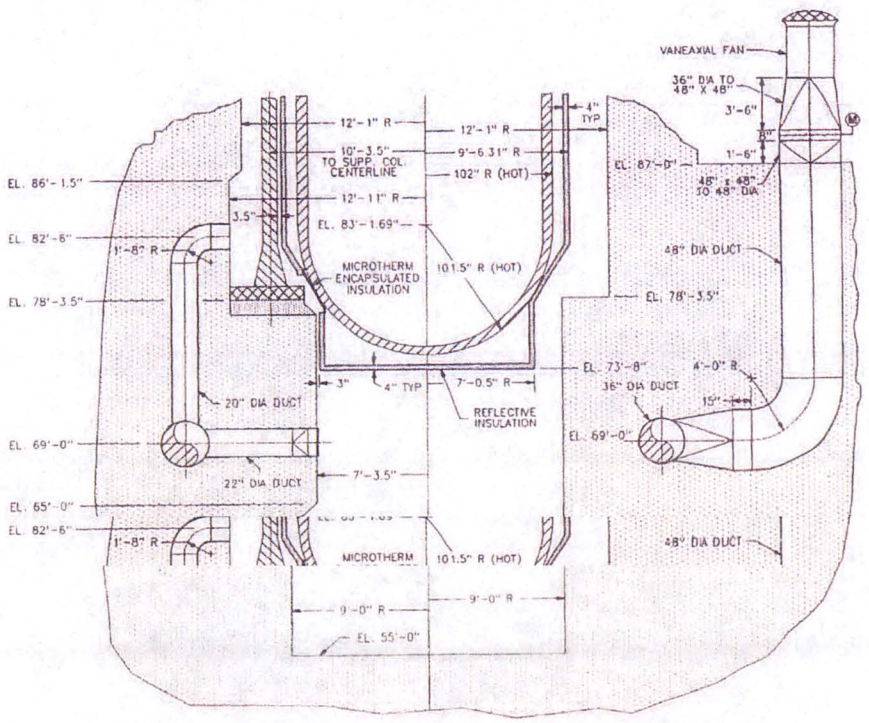

Figure 4-3: Reactor Cavity Normal Cooling Fan Ducts

An approximate distribution of blowdown of Temp-Mat and Microtherm insulation due to RPV nozzle breaks into the three regions described above is based on the relative percentage of flow area among the three locations, see Table 4-7. For example, 225 ft^2 of flow area is 59% of the total (14.7+141.5+225.0 =) 381.2 ft^2 flow area from the RPV nozzle region to the Refueling Cavity, via Piping Penetrations and Reactor Cavity.

Table 4-7: RPV Nozzle Break Flowpaths

Blowdown Path	Flow Area (ft^2)	Percent
Refueling Cavity	14.7	3.9
Piping Penetrations	141.5	37.1
Reactor Cavity	225.0	59.0

From Table 4-7, 41% (Refueling Cavity and Piping Penetration portion) of destroyed Temp-Mat and Microtherm debris blowdown from RPV nozzle breaks will go directly to the D-ring Steam Generator Sub-compartments. The remaining 59% of destroyed Temp-Mat and Microtherm debris blowdown from RPV nozzle breaks will go into the Reactor Cavity.

4.5.2.2 Transport Fractions

The transport fractions for Temp-Mat and Microtherm that is destroyed by RPV nozzle breaks and blows to the D-ring Steam Generator sub-compartments via the Refueling Cavity or Piping Penetration paths are defined by the transport fractions for debris in the D-ring Steam Generator sub-compartments, (i.e., those shown in Table 4-6).

The flowpath from the Reactor Cavity to the ECCS sump strainers consists of two segments. The first segment is flow from the Reactor Cavity to the D-ring Steam Generator sub-compartments. The second segment is flow from the D-ring Steam Generator sub-compartments to the ECCS sump strainers. Consequently, overall transport fractions for destroyed insulation that is transported down into the Reactor Cavity are of the form:

$$f_{TOT} = [\ (Q_{X\,RC} \times f_{X\,RC\text{-}D}) + Q_{X\,D}\ ] \times f_{X\,D} \quad \text{where}$$

f_{TOT} is the overall transport fraction for debris type "X"
$Q_{X\,RC}$ is the quantity of debris type "X" blown down into the Reactor Cavity
$f_{X\,RC\text{-}D}$ is the transport fraction from the Reactor Cavity to the D-ring for debris type "X"
$Q_{X\,D}$ is the quantity of debris type "X" blown down into the D-ring
$f_{X\,D}$ is the transport fraction from the D-ring to the sump strainer for debris type "X"

A computational fluid dynamics (CFD) analysis of recirculation phase steady state flow conditions in the Reactor Cavity at maximum flow entering the RPV annulus and Reactor Cavity was performed. Results of the analysis showed that the maximum turbulent kinetic energy (TKE) in the Reactor Cavity is less than what is required to suspend Nukon Small and Large Pieces. Therefore, $f_{RC\text{-}D}$ for Nukon and Temp-Mat Small and Large Pieces is zero.

Table 4-8 summarizes total transport fractions for Temp-Mat and Microtherm debris blown down to the Reactor Cavity from breaks at RPV nozzles.

Table 4-8: Total Transport Fractions from Reactor Cavity

Insulation	Size	Flow Scenario	f_{RC-D}	f_D	f_{TOT}
Temp-Mat	Fines	all	1.0	1.0	1.0
Temp-Mat	Small Pieces	all	0.0	1.0	0.0
Temp-Mat	Large Pieces	1, 2, 3	0.0	0.0	0.0
Temp-Mat	Large Pieces	5	0.0	1.0	0.0
Microtherm	Fines	all	1.0	1.0	1.0

4.5.3 Temp-Mat Erosion

When using size distributions from Proprietary Alion Report ALION-REP-ALION-2806-01 [15] for Temp-Mat, it is appropriate to assume that Small Pieces and Large Pieces of Temp-Mat that do not transport will be subject to some degree of erosion, which can produce fines that are easily transported. Size distributions from Proprietary Alion Report ALION-REP-ALION-2806-01 [15] are used in Temp-Mat debris transport analysis for RPV nozzle breaks.

Proprietary Alion Report ALION-REP-ALION-I006-04 [16] contains results of erosion testing of small pieces of Low Density Fiberglass (LDFG) debris. Key conclusions reached in the report and the manner in which they apply to Temp-Mat debris transport analysis for RPV nozzle breaks are discussed in ALION-REP-APS-9199-02 [11].

Figure 4-4 illustrates maximum horizontal flow velocity contours at the base of the Reactor Cavity under maximum recirculation phase steady state flow conditions. The velocity in this region where Temp-Mat is expected to collect if destroyed by break jet forces is between 0 and 0.813 ft^2/sec.

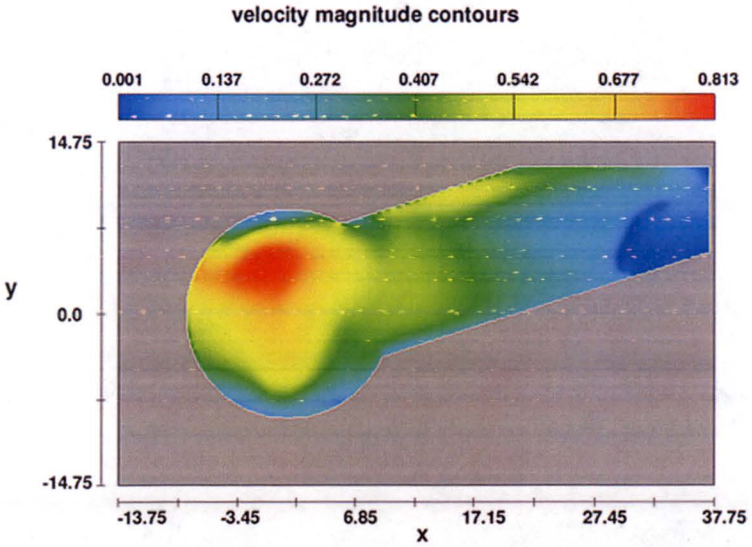

Figure 4-4: Horizontal Flow Velocity Contours at Base of Reactor Cavity

Within this range of flow velocities, some of the Temp-Mat will not tumble because the incipient tumbling velocity is not exceeded (0.12 ft/sec for Small Pieces, NUREG/CR-6772, Table 3.2 [31] and 0.37 ft/sec for Large Pieces, NUREG/CR-6808, Table 5-3 [30]), while some, (i.e., that

portion that is exposed to velocities greater than the incipient tumbling velocity, will tend to tumble).

Those Temp-Mat portions that are able to tumble will experience less erosion than those which are stationary since the former will be moving with the erosive fluid to some degree. The qualifier "some degree" is added because Temp-Mat tumbling may be partially impeded by surrounding destroyed RMI debris, whose incipient tumbling velocities is approximately 0.20 ft/sec to 0.25 ft/sec [20]. However, under sufficiently high velocity, Temp-Mat at the base of the Reactor Cavity will transport (albeit not vertically out to the D-ring Steam Generator sub-compartments) and hence the degree of erosion reported in ALION-REP-ALION-I006-04 [16] will not occur, since the manner in which the Low Density Fiberglass in the erosion tests were secured in the flow flume is not prototypical of the Temp-Mat in the Reactor Cavity.

On the basis of the results in Proprietary Alion Report ALION-REP-ALION-I006-04 [16] and the manner in which they apply to Temp-Mat debris transport analysis for RPV nozzle breaks discussed in ALION-REP-APS-9199-02 [11] and above, the use of a 6% erosion fraction for Small Pieces and Large Pieces of Temp-Mat in the reactor Cavity is justified. However, for added conservatism, an erosion fraction of 10% is used to derive an upper bound of eroded fiber fines.

4.5.3.1 Temp-Mat Debris Transport Results

Table 4-9: Debris Transport Results

Break Case[1]	Break Location[1]	Flow Scenario[1]	Break Scenario Flow Split Factor	Transported Temp-Mat Fines (ft^3)	Transported Temp-Mat Small/Large (ft^3)	Transported E-glass Fiber Fines (ft^3)	Transported Microtherm Particulate (ft^3)
1	S1 (SG2@HL)	5 LPSI on	0.7	0.0	0.0	0.0	0.0
1	S1 (SG2@HL)	5 LPSI off	0.3	0.0	0.0	0.0	0.0
1	S1 (SG2@HL)	1, 2, 3	1.0	0.0	0.0	0.0	0.0
2	RPV CL 2A	5 LPSI on	0.7	1.7	0.3	0.1	10.7
2	RPV CL 2A	5 LPSI off	0.3	0.7	0.1	0.0	4.6
2	RPV CL 2A	1, 2, 3	1.0	2.4	0.0	0.1	15.3
3	RPV HL 2	5 LPSI on	0.7	1.7	0.3	0.1	11.8
3	RPV HL 2	5 LPSI off	0.3	0.7	0.1	0.0	5.0
3	RPV HL 2	1, 2, 3	1.0	2.5	0.0	0.2	16.8

Note:
1. See break location and flow descriptions in Section 4.4.5

4.5.3.2 Total Fiber Transport Results

Table 4-10 contains a summary of the total quantity of fiber postulated to transport to the sump strainer for each analysis case.

Table 4-10: Total Fiber Transport Results

Break Case[1]	Break Location[1]	Flow Scenario[1]	Transported Small/Fine Fiber from Temp-Mat[2] (ft^3)	Transported E-glass Fiber Fines (ft^3)[4]	Transported Small/Fine Fiber from AoR (ft^3)	Latent Fiber[3] (ft^3)	Transported Large Fiber from Temp-Mat[1] (ft^3)	Transported Large Fiber from AoR[2] (ft^3)	Total Fiber Transported all sizes (ft^3)
1	S1 (SG@HL)	5 LPSI on	0.0	0.0	4.1	8.8	0.0	2.8	15.6
1	S1 (SG@HL)	5 LPSI off	0.0	0.0	1.8	3.8	0.0	1.2	6.7
1	S1 (SG@HL)	1, 2, 3	0.0	0.0	5.9	12.5	0.0	0.0	18.4
2	RPV CL 2A	5 LPSI on	8.4	0.1	0.0	8.8	1.6	0.0	18.8
2	RPV CL 2A	5 LPSI off	3.6	0.0	0.0	3.8	0.7	0.0	8.0
2	RPV CL 2A	1, 2, 3	11.9	0.1	0.0	12.5	0.0	0.0	24.6
3	RPV HL 2	5 LPSI on	8.5	0.1	0.0	8.8	1.6	0.0	18.9
3	RPV HL 2	5 LPSI off	3.6	0.0	0.0	3.8	0.7	0.0	8.1
3	RPV HL 2	1, 2, 3	12.1	0.2	0.0	12.5	0.0	0.0	24.8

Notes:
1. See break location and flow descriptions in Section 4.4.5
2. Fiber content in Temp-Mat volume takes into account the difference in density between Temp-Mat and Nukon.
3. Transport of AoR quantities for "c" cases are 70% and 30% of total to reflect Flow Scenario 5 70/30 flow split.
4. E-glass quantity is 0.0096 ft^3 E-Glass/ ft^3 Transported Microtherm [11].

4.5.3.3 Evaluation of Temp-Mat Transport Results

The objective of the planned removal of newly-discovered Temp-Mat is to maintain the total quantity of fiber transported to the sump at or below the quantity that was used in the headloss Test of Record.

Table 4-11 contains a summary of fiber loading from the Analyses of Record and the Test of Record.

Table 4-11: Original Calculated versus Tested Fibrous Debris Quantities

Description	**Units**	**Quantity Transported to Sump Strainer by Analysis** [20]	**Quantity Used in Strainer Testing** [20], [22]
Nukon – Fines / Small Pieces	ft^3	5.89	8.31
Nukon – Large Pieces	ft^3	3.93	5.54
Latent Debris – Fiber (Fines)	ft^3	12.5	12.5
Total Fines / Small Pieces	ft^3	18.39*	20.81*

* Sum of Nukon Fines/Small Pieces and Latent Debris only; Fines/Small sum excludes Large Pieces

Table 4-12 provides a comparison between the total new/current fibrous debris quantities transported to the sump strainer versus the fibrous debris quantities used in the test-of-record (ToR) strainer prototype headloss testing per the test specification, N001-1106-00229 [22]

Since the purpose of this comparison is to assess the impact of new Temp-Mat on headloss, and since headloss test quantities in testing were entered on a mass basis, Temp-Mat quantities are factored to enable a mass quantity comparison.

The total new Small/Fine fibrous debris quantity shown in Table 4-12 is computed as follows:

$$Q_{NEW\text{-}fib} = [\, Q_{NEW\ T\text{-}M} + Q_{AoR\text{-}fib} + Q_{LATENT\text{-}fib} \,], \text{ where:}$$

$Q_{NEW\text{-}fib}$ is the <u>total</u> new transported fiber quantity
$Q_{NEW\ T\text{-}M}$ is the newly-discovered Temp-Mat that transports to the sump strainers (Table 4-9)
$Q_{AoR\text{-}fib}$ is the quantity of fiber determined to transport to the sump strainer in the Analysis-of-Record (AoR), which for RPV break cases is zero, and
$Q_{LATENT\text{-}fib}$ is the quantity of latent fiber that transports to the sump strainers

$Q_{AoR\text{-}fib}$ is 5.89 ft^3 for Small/Fine fibrous debris [20]
$Q_{AoR\text{-}fib}$ is 3.93 ft^3 for Large Piece fibrous debris [20]
$Q_{LATENT\text{-}fib}$ is 12.5 ft^3 (Small/Fine) fibrous debris

The ratio in Table 4-10 is $Q_{NEW\text{-}fib} / Q_{ToR}$, where:

Q_{ToR} is the <u>total</u> quantity of fiber used in the ToR, including the portion that represents latent fiber.

Q_{ToR} for Small/Fine fiber is 8.31 ft^3 Nukon plus 12.5 ft^3 latent fiber.

The total new Large fibrous debris quantity comparison versus the Test of Record (ToR) is a direct comparison of Large-only quantities. Q_{ToR} for Large Piece fiber is 5.54 ft^3 Nukon. The Temp-Mat quantity is factored to provide a mass quantity comparison.

Table 4-12: Comparison of Current Versus ToR Fiber Loading

Break Case[1]	Break Location[1]	Flow Scenario[1]	Total Fiber Fine or Small/Fine New / ToR ratio	Total Fiber Large New / ToR ratio	Total Fiber all sizes New / ToR ratio
1	S1 (SG2@HL)	5 LPSI on	0.62	0.50	0.59
1	S1 (SG2@HL)	5 LPSI off	0.27	0.22	0.25
1	S1 (SG2@HL)	1, 2, 3	0.88	0.00	0.70
2	RPV CL 2A	5 LPSI on	0.83	0.29	0.67
2	RPV CL 2A	5 LPSI off	0.35	0.12	0.28
2	RPV CL 2A	1, 2, 3	1.18	0.00	0.87
3	RPV HL 2	5 LPSI on	0.83	0.29	0.67
3	RPV HL 2	5 LPSI off	0.36	0.12	0.29
3	RPV HL 2	1, 2, 3	1.19	0.00	0.87

1. See break location and flow descriptions in Section 4.4.5

Results in Table 4-12 show that the total fiber associated with all breaks for the configuration after planned Temp-Mat removal is less than the total fiber used in the ToR. The quantity of Fines/Smalls associated with the configuration after planned Temp-Mat removal, is less than or within 19% of the total fiber used in the Test of Record.

4.6 Chemical Effects

WCAP-16530-NP spreadsheet was used to estimate the chemical particulate quantities associated with the analysis cases that represent the current condition, after planned Temp-Mat removal is accomplished. The fiber and Microtherm inputs and resulting total quantity of chemical particulate quantities from WCAP-16530-NP spreadsheet calculations are presented in Table 4-13. Also presented in Table 4-13 is the "normalized" total precipitate quantity. "Normalized" total precipitate quantity is defined as current condition precipitate quantity divided by the net surface area per strainer, i.e., 2742 ft^2 per strainer train.

Table 4-13: Selected Inputs and Results of Chemical Precipitate Calculations

Break Case[1]	Flow Scenario[1]	Break Location[1]	Total Latent Fiber[5] (ft^3)	Total Nukon[3,5,6] (ft^3)	Total Temp-Mat[5] (ft^3)	Total Micro-therm[2,5] (ft^3)	Total Precipitate (lbm)	Normalized Total (lbm/ft^2)[4]
1	5 LPSI on	S1 (SG2@HL)	5.25	6.87	6.0	2.9	140.9	0.051
1	5 LPSI off	S1 (SG2@HL)	2.25	2.95	2.6	1.3	101.0	0.037
1	1, 2, 3	S1 (SG2@HL)	7.5	9.82	8.6	4.2	171.6	0.063
2*	5 LPSI on	RPV CL 2A	5.25	6.92	8.0	13.6	205.1	0.075
2*	5 LPSI off	RPV CL 2A	2.25	2.95	3.4	5.8	128.4	0.047
2*	1, 2, 3	RPV CL 2A	7.5	9.97	11.4	19.5	262.8	0.096
3	5 LPSI on	RPV HL 2	5.25	6.93	8.0	14.7	205.1	0.075
3	5 LPSI off	RPV HL 2	2.25	2.95	3.4	6.3	128.4	0.047
3	1, 2, 3	RPV HL 2	7.5	9.98	11.4	21.0	262.8	0.096

* Results for case 2 are based on case 3 inputs, which are bounding.

Notes:
1 See break location and flow descriptions in Section 4.4.5
2 Microtherm density:15 lb/ft^3 [11]
3 For RPV break cases, assumes that all S1 Nukon (9.82 = 5.89 + 3.93; Small/Fines, Large Pieces, resp. [20]) is affected by spray
4 Normalized chemical total is based on net surface area per strainer is 2742 ft^2 [22]
5 Quantities for cases a, c and e are 70% and 30% of total to reflect Flow Scenario 5 70/30 flow split
6 Nukon values include transported E-glass associated with Microtherm and eroded Temp-Mat fines for RPV break cases

The maximum normalized quantity of chemical precipitate for the current condition, after planned Temp-Mat removal is accomplished, is 0.096 lb/ft^2, which is less than the normalized quantity of chemical precipitate used in the headloss Test of Record [21], 0.0997 lb/ft^2.

4.7 Strainer Headloss

4.7.1 D-ring Steam Generator Sub-compartment Breaks

Once the Temp-Mat removal itemized in Table 3-1 is accomplished, all three Units will be restored to the condition that was described in Revision 2 of APS Supplemental Response to GL 2004-02 for breaks in the D-ring Steam Generator Sub-compartment. As before, the S1 break will be the governing D-ring break. The fiber quantities associate with the S1 break will be restored to those in the Analysis of Record; the maximum headloss associated with D-ring breaks (which do not include any transport of Microtherm) will be restored to those documented in N001-1106-00247 [24].

4.7.2 RPV Nozzle Breaks

4.7.2.1 RPV Nozzle Breaks – General Approach

The PVNGS headloss Test of Record (ToR) did not address Microtherm debris. Therefore it is not possible to estimate maximum headloss with the presence of Microtherm based solely on PVNGS headloss Test of Record results. However, other plants with CCI strainers conducted testing that included microporous insulation debris, (e.g., Min-K and Cal-Sil). In particular, testing performed by Salem Nuclear Generating Station, included Min-K [39]. Table 4-14 provides a comparison of PVNGS RPV break headloss-related parameters associated with Flow Scenarios S1, S2 and S3 ; Flow Scenario S5 for the train with 11,600 gpm flow (LPSI on, 70% flow), Flow Scenario S5 for the train with 6,600 gpm flow (LPSI off, 30% flow) versus Salem Unit 2, Test 6 (S2T6). Both absolute values and normalized values are provided. The normalized values are per net strainer surface area, (e.g., normalized fiber quantity is lbm/sq-ft).

Table 4-14: Comparison of PVNGS RPV Break and S2T6 Parameters

Item #	Parameter	Units	PV Flow Cases 1, 2 & 3	PV Flow Case 5 (LPSI on, 70%)	PV Flow Case 5 (LPSI off, 30%)	Salem Unit 2 Test 6	PV123 ------- S2T6	PV5(70%) ---------- S2T6	PV5(30%) ---------- S2T6
	Strainer Flow								
1	Approach Velocity	ft/s	0.0617	0.1085	0.0617	0.0552	112%	197%	112%
	Debris Load								
2	Fiber [1]	lbm	59.4	45.3	19.4	497.1			
3	Particulate [2]	ft^3	12.73	8.91	3.82	13.00			
4	Microtherm [3]	lbm	252.3	176.6	75.7	n/a			
5	Min-K	lbm	n/a	n/a	n/a	392.0			
6	Chemical (max from calcs)	lbm	262.8	205.1	128.4	511.0			
7	Theoretical Bed Thickness	in	0.11	0.08	0.03	0.30	36%	26%	11%
	Normalized Debris Load								
8	Fiber	lbm/ft^2	0.052	0.040	0.017	0.120	43%	33%	14%
9	Particulate	ft^3/ft^2	0.0046	0.0032	0.0014	0.0031	150%	105%	45%
10	Microtherm	lbm/ft^2	0.092	0.064	0.028	n/a	Microtherm/Min-K		
11	Min-K	lbm/ft^2	n/a	n/a	n/a	0.094	98%	69%	29%
12	Chemical	lbm/ft^2	0.096	0.075	0.047	0.123	78%	61%	38%
13	Open Area	n/a	yes	yes	yes	no			

Notes:

1 Maximum total transported (Small/Fine + Large Pieces + Latent) in PVNGS cases that represent the new design configuration after recommended insulation removal. Fiber density is 2.4 lb/ft^3; Temp-Mat mass quantity reflects Temp-Mat's higher density.

2 N001-1106-00247 [24]

3 Microtherm Density: 15.0 lbm/ft^3 [11]

4.7.2.2 RPV Nozzle Breaks – Evaluation of Fibrous Debris

The Enclosure *Review of NEI Low Fiber Plant Resolution Criteria* in NRC Letter (ADAMS ML120730181) to NEI [40] states in part:

> "The staff finds that plants that have redundant strainers installed may credit the entire strainer area of all strainers, with the exception of sacrificial area for miscellaneous debris, provided the plant procedures direct the prompt restoration of the remaining trains to service or there is other justification for crediting the total surface area. This position considers that although design bases may require one strainer or train to be considered failed, licensees will take all actions necessary to return the out of service train to service in a reasonable period of time. The staff determined that any significant head losses would develop over relatively long periods of time such that licensees could take actions to return required equipment to service."

Step 5 of Section 3.0, Instructions / Contingency Actions in PVNGS *Loss Of Coolant Accident* procedure 40EP-9EO03, [41], states in part:

> "IF SIAS has actuated, THEN perform the following: a. Check that the HPSI and LPSI Pumps have started." and "a.1 Start idle HPSI and LPSI Pumps as necessary."

PVNGS procedure 40EP-9EO03 [41], actions are consistent with NRC expectations of licensee actions. As a result, it is justified to create the fiber to strainer area metric used in the NRC letter [40] based on total net strainer area. The net surface area of each strainer is 2742 ft^2 [22]. Therefore the total net strainer area at PVNGS is 5484 ft^2, (2 x 2742 ft^2). The maximum total quantities of transported fiber debris, consisting of existing Nukon, Temp-Mat (directly destroyed and transported and transported eroded fines), E-glass from destroyed Microtherm and Latent Fiber for each condition are summarized in Table 4-10.

4.7.2.3 RPV Nozzle Breaks – Flow Scenarios 1, 2 and 3 (LPSI Secured)

Total maximum fiber, including existing Nukon, Temp-Mat (directly destroyed and transported and transported eroded fines), E-glass from destroyed Microtherm and Latent Fiber is 24.8 ft^3 (see Table 4-10). Fiber metric is:

$$(24.8\ ft^3 / 5484\ ft^2) \times 12\ inch/ft = 0.054\ inch;$$ which is less than 1/16 inch

The NRC letter [40] states that in the absence of problematic insulation types, e.g., Microtherm, Min-K and Cal-Sil, plants with less than 1/16 inch fiber "...head loss test will not be required ..."; (i.e., there is insufficient fiber to be of concern). Since APS has discovered Microtherm at PVNGS, a portion of which is expected to transport to the sump strainer, additional assessment is required, and is discussed below.

Table 4-15 contains a direct comparison of maximum normalized strainer debris loads for PVNGS for cases that represent the new design configuration after recommended insulation removal for Flow Scenarios 1, 2 and 3 versus results of Salem Unit 2 Test 6. Other pertinent parameters are also listed. The information in Table 4-15 is obtained from Table 4-14.

Table 4-15: Comparison of PVNGS and S2T6 Parameters, Flow Scenarios 1, 2 and 3

Parameters	Units	PV Flow Cases 1, 2 & 3	Salem 2 Test 6	PV123 ------- S2T6
Fiber	lbm/ft^2	0.052	0.120	43%
Particulate	ft^3/ft^2	0.005	0.003	150%
Microporous Insulation	lbm/ft^2	0.092	0.094	98%
Chemical	lbm/ft^2	0.096	0.123	78%
Strainer Approach Velocity	ft/s	0.0617	0.0552	112%
Open Area	n/a	yes	no	

Table 4-15 illustrates that fiber, microporous and chemical debris loading for S2T6 bound PVNGS. The approach velocities are nearly equal, within 12%. PVNGS had observed open/clean strainer surface area; S2T6 did not. As stated in N001-1106-00247 [24], fiber debris is necessary to create the "mat" upon which particulate debris is deposited. Additional debris laden area on the strainer is not expected because the overall quantity of fiber for these cases are less than those considered in the Test-of-Record and fiber fines are below or within 19% of the Test-of-Record. Given the significantly greater fiber and chemical loads for S2T6, it is considered that headlosses for S2T6 are greater than for PVNGS.

4.7.2.4 RPV Nozzle Breaks – Flow Scenario 5 (Train at which LPSI is Not Secured)

Total maximum fiber, including existing Nukon, Temp-Mat (directly destroyed and transported and transported eroded fines), E-glass from destroyed Microtherm and Latent Fiber associated with the strainer at which LPSI is not secured after RAS is 18.9 ft^3, see Table 4-10. Fiber metric is:

$$(18.9\ ft^3 / 5484\ ft^2) \times 12\ inch/ft = 0.041\ inch;\ which\ is\ less\ than\ 1/16\ inch$$

Table 4-16 contains a direct comparison of maximum normalized strainer debris loads for PVNGS for cases that represent the new design configuration after recommended insulation removal for Flow Scenario 5 versus results of Salem Unit 2 Test 6. Other pertinent parameters are also listed. The information in Table 4-16 is obtained from Table 4-14.

Key parameters for assessment of this case are the small fiber quantity and open/clean strainer surface for PVNGS and the significant difference in approach velocity, where the approach velocity for PVNGS is nearly twice that of S2T6.

Table 4-16: Comparison of PVNGS and S2T6, Flow Scenario 5, LPSI Non-Secured

Parameters	Units	PV Flow Case 5	Salem 2 Test 6	PV123 ------- S2T6
Fiber	lbm/ft^2	0.040	0.120	33%
Particulate	ft^3/ft^2	0.003	0.003	105%
Microporous Insulation	lbm/ft^2	0.064	0.094	69%
Chemical	lbm/ft^2	0.075	0.123	61%
Strainer Approach Velocity	ft/s	0.1085	0.055	197%
Open Area	n/a	yes	no	

Table 4-16 illustrates that fiber, microporous and chemical debris loading for S2T6 bound PVNGS. Normalized particulate loads are approximately equal, within 5%. Although the approach velocity in the PVNGS case is nearly twice that of S2T6, 197%, PVNGS had observed open/clean strainer surface area; S2T6 did not. Given the significantly greater fiber and chemical loads for S2T6, it is considered that headlosses for S2T6, even with the higher PVNGS approach velocity, are greater than for PVNGS.

4.7.2.5 RPV Nozzle Breaks – Flow Scenario 5 (Train at which LPSI is Secured)

The maximum fiber, including existing Nukon, Temp-Mat (directly destroyed and transported and transported eroded fines), E-glass from destroyed Microtherm and Latent Fiber associated with the strainer at which LPSI is not secured after RAS is 8.1 ft^3, see Table 4-10. Fiber metric is:

$$(8.1\ ft^3 / 5484\ ft^2) \times 12\ inch/ft = 0.018\ inch;\ which\ is\ less\ than\ 1/16\ inch$$

Table 4-17 contains a direct comparison of maximum normalized strainer debris loads for PVNGS for cases that represent the new design configuration after recommended insulation removal for Flow Scenario 5 versus results of Salem Unit 2 Test 6. Other pertinent parameters are also listed. The information in Table 4-17 is obtained from Table 4-14 and Table 4-10.

Key parameters for assessment of this case are the small fiber quantity and open/clean strainer surface for PVNGS and the small difference in approach velocity (12%) between PVNGS and S2T6.

Table 4-17: Comparison of PVNGS and S2T6, Flow Scenario 5, LPSI Secured

Parameters	Units	PV Flow Case 5	Salem 2 Test 6	PV123 ------- S2T6
Fiber	lbm/ft^2	0.017	0.120	14%
Particulate	ft^3/ft^2	0.001	0.003	45%
Microporous Insulation	lbm/ft^2	0.028	0.094	29%
Chemical	lbm/ft^2	0.029	0.123	38%
Strainer Approach Velocity	ft/s	0.0617	0.055	112%
Open Area	n/a	yes	no	

Table 4-17 illustrates that the non-chemical and chemical debris loading for S2T6 bound PVNGS. The approach velocities are nearly equal, within 12%, and PVNGS had observed open/clean strainer surface area; S2T6 did not. Given the significantly greater fiber and chemical loads for S2T6, it is considered that headlosses for S2T6 are greater than for PVNGS.

4.7.2.6 Design Basis Headloss

The discussion in Sections 4.7.2.3, 4.7.2.4 and 4.7.2.5 indicates that the maximum headloss for PVNGS RPV nozzle breaks is no greater than the headlosses determined from S2T6. There is no reliable method for estimating the amount by which S2T6 headloss exceeds corresponding PVNGS headloss. Therefore, for purposes of establishing design headloss for PVNGS, for cases where S2T6 exceed PVNGS ToR values, the S2T6 headloss is assigned as the new design headloss for PVNGS. Table 4-18 provides a summary of maximum headloss from the original ToR, headloss results from Salem Unit 2, Test 6 [28], the new design headloss for PVNGS, the overall strainer headloss limit developed in Section 4.2.2 and the headloss margin.

Table 4-18: Summary of Design Headloss, Limits and Margin

Temp [6] (°F)	Total ΔP [1] Flow Cases 1, 2, 3 (ft-Water)	Total ΔP [1] Flow Case 5 (ft-Water)	S2TS Debris Headloss [2] (ft-Water)	Design Headloss [3] (ft-Water)	Overall Strainer Limit [4] (ft-Water)	Headloss Margin (ft-Water)
77	5.13	9.28	9.78	9.78	12.00	2.22
86	4.91	8.74	9.78	9.78	12.00	2.22
104	4.50	7.78	9.78	9.78	12.00	2.22
122	4.10	6.89	9.78	9.78	12.00	2.22
140	3.70	6.07	9.78	9.78	12.00	2.22
158	3.47	5.60	9.78	9.78	12.00	2.22
160	3.45 [5]	5.56 [5]	9.78	9.78	12.00	2.22
170	3.33 [5]	5.34 [5]	3.21	5.34	12.00	6.66
174.9	3.27	5.23	3.21	5.23	9.25	4.02
175	3.27	5.23	3.10	5.23	9.25	4.02
176	3.26	5.20	3.10	5.20	9.23	4.03
179.78	3.22	5.12	3.08	5.12	9.18	4.06
180	3.22	5.12	2.99	5.12	9.17	4.05
193.8	3.07	4.84	less than 2.99	4.84	7.71	2.27
252	2.58	3.95	less than 2.99	3.95	7.93	3.98

Notes:
1. N001-1106-00247 [42]
2. Salem Generating Station, Units 1 and 2, Final Supplemental Response [28]
3. Maximum of PVNGS ToR and S2T6 headloss values in adjacent columns
4. From Table 4-1, developed in Section 4.2.2
5. Value is based on linear interpolation between published values
6 Temperature value decimal places are intentionally different, designed to be exactly the same as used in associated reference documents

The new Design Headloss and the governing Overall Strainer Limit over the temperature range of 77° F to 152° F, shown in Table 4-18 above, are illustrated in Figure 4-5.

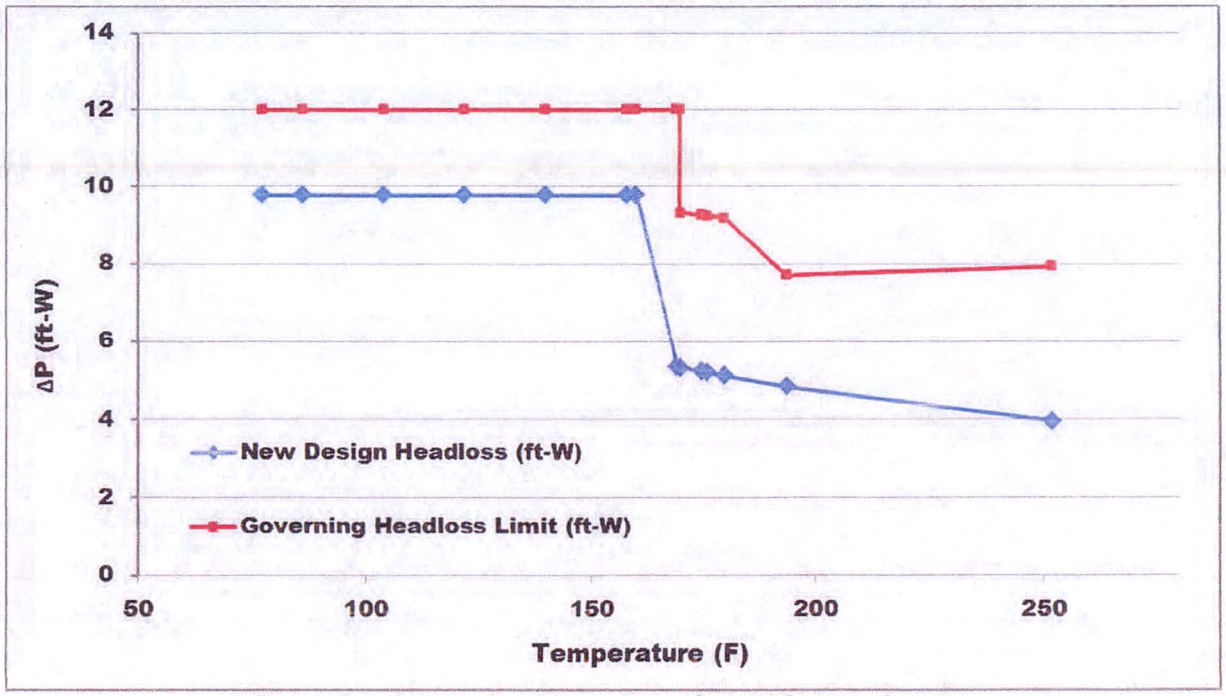

Figure 4-5: Design Headloss versus Overall Strainer Limit

4.7.2.7 Design Basis Fiber Limit

The basis for determining that the headloss results determined in S2T6 testing are applicable and bounding is in part based on the comparisons of total transported fiber to the sump strainers, as discussed in Sections 4.7.2.3, 4.7.2.4 and 4.7.2.5. The applicable threshold transported fiber quantities upon which the determination in Sections 4.7.2.3, 4.7.2.4 and 4.7.2.5 are based are summarized in Table 4-19.

Table 4-19: Design Basis Fiber Limit

Transported Fiber Description	Design Basis Value (cu-ft)	Basis
Total fiber, all sizes, all breaks, including Latent Debris and E-glass	26.35	Test of Record, see Table 4-11
Total Small/Fine fiber, including Latent Debris and E-glass, for D-ring Breaks	20.81	Test of Record, see Table 4-11; Section 4.7.2.3
Total fiber Fines, including Latent Debris and E-glass for RPV Breaks	24.80	Comparative Analysis in Sections 4.7.2.3, 4.7.2.4 and 4.7.2.5

4.8 Downstream Effects

4.8.1 In-Vessel

The mass of bypass fiber reported in Revision 2 to the APS Supplemental Response is 12.8 grams per fuel assembly [10]. The 12.8 grams per fuel assembly result is documented in [43]. Table 4-20 provides a comparison of the bypass fiber mass per fuel assembly reported in Revision 2 to the APS Supplemental Response (column A) versus the new design configuration after recommended insulation removal (column B). The maximum total Nukon-equivalent fiber quantity for the current recommended configuration in column B is obtained from Table 4-10.

Table 4-20: Grams of Bypass Fiber per Fuel Assembly

Item	R2 Supplemental Response (column A)	Updated (column B)	Units
NUKON-EQUIV FIBER			
Total Nukon (Fine/Small and Large)	9.82	---	ft^3
Total Latent Fiber	12.50	---	ft^3
Total Nukon-equivalent fiber	22.32	24.8	ft^3
Total Nukon- equivalent fiber	53.57	59.52	lb
ALPHA CLOTH			
Total 16 lb/ft^3 Alpha Cloth	0.10	0.00	ft^3
Total Alpha Cloth	1.60	0.00	lb
FIBER LOAD OF FUEL ASSEMBLIES			
Total Mass of Fibrous Debris	55.17	59.52	lb
Bypass Fraction	12.3%	12.3%	
Total Mass of Bypass Fibrous Debris	6.79	7.32	lb
Conversion Factor	453.59	453.59	grams/lb
Total Mass of Bypass Fibrous Debris	3077.92	3320.73	grams
Fuel Assemblies (FA)	241	241	
Grams of Bypass Fiber per Fuel Assembly	12.8	13.8	grams/FA

At this time, all Alpha Cloth has been removed from all areas that are subject to pipe breaks that require ECCS actuation. The results in Table 4-20 show that for the new design configuration after recommended insulation removal, the fiber load is 13.8 grams per fuel assembly, which is less than the 15 grams per fuel assembly limit in WCAP-16793-NP [44], which is cited in Revision 2 to the APS Supplemental Response [10] as an acceptance criterion.

4.8.2 Ex-Vessel Equipment Wear

A list of the equipment that is potentially subject to wear from post-LOCA particulate debris, including Microtherm resulting from RPV nozzle breaks is summarized in Table 4-21. Also listed in Table 4-21 are the documents that contain the evaluations that were performed and the key technical references that support the evaluations.

Table 4-21: Ex-Vessel Equipment Wear Evaluation Basis

EQUIPMENT DESCRIPTION	EWR	ANALYTICAL REFERENCE DOCUMENT(S)
ECCS Pump Seal Cyclone Separators	EWR 4746166 [45]	N001-1106-00225, Evaluation of Effects of Debris on the Palo Verde ECCS Pump Seal Cyclone Separators [33]
		N001-1106-00012, Palo Verde Sump Debris Downstream Effects Evaluation for ECCS Equipment [34] (abrasive wear)
		N001-1106-00011, Palo Verde Units 1, 2, and 3 GSI-191 Down-Stream Effects Debris Ingestion Evaluation [35] (erosive wear and erosion)
ECCS Equipment and Valves	EWR 4746165 [46] and WEC Letter LTR-SEE-16-103 [47]	N001-1106-00013, Palo Verde Sump Debris Downstream Effects Evaluation for ECCS Valves [36]
		N001-1106-00012, Palo Verde Sump Debris Downstream Effects Evaluation for ECCS Equipment [34](abrasive wear)
		N001-1106-00011, Palo Verde Units 1, 2, and 3 GSI-191 Down-Stream Effects Debris Ingestion Evaluation [35] (erosive wear and erosion)

It is concluded in both EWRs that Microtherm is equivalent to a small, 10 micron inorganic zinc particles. Based on the fact that abrasive wear is conservatively assumed to occur with particles larger than 50 microns [34], Microtherm does not add to abrasive wear. Therefore existing analyses related to the ECCS Pump Seal Cyclone Separators and ECCS equipment and valves remain bounding.

It is concluded in both EWRs that the maximum revised coating mass concentration, including Microtherm contribution from Reactor Vessel Nozzle breaks is 403 ppm. This value compares favorably with the previously analyzed value of 982 ppm for the wear evaluations. Therefore existing analyses related to the ECCS Pump Seal Cyclone Separators and ECCS equipment and valves remain bounding.

4.9 Vortex Formation

The potential for formation of vortices in the event of pump stopping and restarting is addressed in Section 9.1.2 of N001-1106-00228 [26]. The headloss across the sump strainer upon which the potential for formation of vortices is based is derived from the original differential pressure structural limit across the strainer, 10.4 feet-water. The maximum design headloss for all pipe break cases for the configuration that results after removal of the insulation described in Table 3-1 is 9.78 feet-water, as shown in Table 4-18, which is less than the 10.4 feet-water used in the analysis of record, N001-1106-00228 [26]. Therefore, there is no potential for formation of vortices in the event of pump stopping and restarting in the current design configuration.

4.10 Flashing Downstream of the Sump Strainer

The potential for flashing downstream of the sump strainer is addressed in Section 9.2 of N001-1106-00228 [26]. The discussion in Section 9.2 of N001-1106-00228 shows that for all flow scenarios and over the temperature range of interest, absolute pressure downstream of the sump strainer is always much higher than the vapor pressure. The discussion in Section 9.2 of N001-1106-00228 demonstrates that the minimum pressure difference between the containment and the vapor pressure of the sump water is 31.8 ft-water, which is significantly higher than the maximum design headloss for all pipe break cases for the configuration that results after removal of the insulation described in Table 3-1, 9.78 feet-water, as shown in Table 4-18. Therefore, there is no potential for flashing downstream of the sump strainer in the current design configuration.

4.11 Air Ingestion Due to Deaeration

The potential for air ingestion due to deaeration at the sump strainer is addressed in Section 9.3 of N001-1106-00228 [26]. The discussion in Section 9.3 of N001-1106-00228 states, in part, that the static water head from the containment pool water surface to the elevation of the pumps suction nozzles is 10 ft – 11 inches, which is greater than the original limiting strainer headloss value, which was chosen to be the original differential pressure structural limit across the strainer, 10.4 feet-water. The maximum design headloss for all pipe break cases for the configuration that results after removal of the insulation described in Table 3-1 is 9.78 feet-water, as shown in Table 4-18, which is less than the 10.4 feet-water used in the analysis of record, N001-1106-00228 [26]. Therefore, any deaeration that could occur in the strainer cavities is reversed before the water reaches the sump outlet. The net air production, therefore, is zero and hence deaeration is not an issue over the temperature range of interest for the configuration that results after removal of the insulation described in Table 3-1.

5 Summary of Results

5.1 D-ring Steam Generator Sub-compartment Breaks

After removal of the insulation described in Table 3-1, the condition described in Revision 2 to the APS Supplemental Response [1] will be restored for breaks in the D-ring Steam Generator Sub-compartments.

5.2 RPV Nozzle Breaks

After removal of the insulation described in Table 3-1, the new, governing debris generation, debris transport, total chemical effects precipitate load, headloss and in-vessel and ex-vessel downstream effects will be as summarized in Table 4-5, Table 4-10, Table 4-13, Table 4-18, Table 4-20 and the discussion in section 4.8.2, respectively. The governing condition is the double-ended guillotine break (DEGB) at the Hot Leg RPV nozzle.

For RPV nozzle breaks, the fiber design limit is defined by the normalized value in Table 4-15. For RPV nozzle breaks (as well as breaks in the D-ring Steam Generator Sub-compartments) the total design chemical effects precipitate load is based on the Test of Record [21].

The assessment described in this document shows that for the configuration that results after removal of the insulation described in Table 3-1, the acceptance criteria discussed in Section 4.3 (i.e., NPSH margin, structural capacity and downstream effects), are satisfied for D-ring and RPV nozzle breaks.

5.3 Vortex Formation, Flashing and Deaeration

For all pipe break locations, over the temperature range of interest, the discussion is Sections 4.9, 4.10 and 4.11 shows that vortex formation, flashing and deaeration, respectively, are not issues for the configuration that results after removal of the insulation described in Table 3-1.

6 Conclusion

After removal of the insulation described in Table 3-1, based on consideration of sump strainer headloss and downstream effects, post-LOCA ECCS operation will not be compromised in the event of DEGB in either the D-ring Steam Generator Sub-compartments or at RPV nozzles. Therefore, as stated in the Overall Compliance Section 3.3, considering the overall parameters for debris generation, debris transport, chemical effects, downstream effects, in-vessel effects, testing methodology, strainer performance testing, increased structural capacity determination [18] and the resulting minimum (of NPSH and structural) margin of 2.22 ft-water, APS has demonstrated the objectives of GL 2004-02 are satisfied for PVNGS Units 1, 2 and 3.

7 References

[1] APS Letter 102-06805, *Revision 2 to Supplemental Response to NRC Generic Letter 2004-02*, dated 18-DEC-2013

[2] APS Condition Report 15-01860

[3] APS-NRC 10-JUN-2015 Meeting Summary (ADAMS Accession Numbers ML15239B322)

[4] APS-NRC 10-JUN-2015 Meeting Presentation Slides (ADAMS Accession Numbers ML15156B352)

[5] APS-NRC 26-AUG-2015 Meeting Summary (ADAMS Accession Nos. ML15268A131).

[6] APS-NRC 26-AUG-2015 Meeting Presentation Slides (ADAMS Accession Numbers ML15236A134)

[7] APS-NRC 17-DEC-2015 Meeting Notice and Agenda, (ADAMS Accession Number ML15328A379)

[8] APS-NRC 17-DEC-2015 Meeting Presentation Slides (ADAMS Accession Number ML15348A054)

[9] APS-NRC 7-SEP-2016 Meeting Presentation Slides (ADAMS Accession Number ML16253A411)

[10] APS Supplemental Response to GL 2004-02, Revision 2 (ADAMS Accession Number ML13357 A218)

[11] ALION-REP-APS-9199-02, *Technical Report: Assessment of Microtherm Insulation In the Palo Verde Reactor Cavities*

[12] Engineering Evaluation ENG WO # 4719679

[13] NEDO-32686-A, Revision 0, *Utility Resolution Guidance for ECCS Suction Strainer Blockage, BWROG*

[14] Sargent and Lundy Evaluation Number 2007-19863, Revision 4, *Post-LOCA Fuel Deposition Analysis in Support of GSI-191*

[15] Proprietary Alion Report ALION-REP-ALION-2806-01 (See ADAMS Accession Number ML14052A053)

[16] Proprietary Alion Report ALION-REP-ALION-I006-04, Revision 1, (See ADAMS Accession Number ML101540221)

[17] N001-1106-00176, Revision 1, *Evaluation of the Maximum Allowable Pressure Difference (of Palo Verde Sump Strainers)*

[18] LTR-AVR-2K16-01-09 *CCI Structural Capacity*

[19] N001-1106-00002–DG, Revision 5, (S&L) *Debris Generation Due to LOCA within Containment for Resolution of GSI-191*

[20] N001-1106-00003–DT, Revision 3, (S&L) *Post-LOCA Debris Transport for Resolution of GSI-191,* Calculation Number 2005-09080

[21] N001-1106-00231, Revision 2, WCAP-16530, (S&L) *Post-LOCA Chemical Effects Analysis in Support of GSI-191*

[22] N001-1106-00229, Revision 2, (CCI) *Chem Effects Test (Spec), Chemical Effect Head Loss Test Specification*

[23] N001-1106-00227, Revision 5, (CCI) *Chem Effects Test (Report), Chemical Effects Test*

[24] N001-1106-00247, Revision 0, *Determination of Head Loss Bump-Up Factor For ECCS Strainers*

[25] N001-1106-00003–DT, Revision 2, (S&L) *Post-LOCA Debris Transport for Resolution of*

GSI-191, Calculation Number 2005-09080

[26] N001-1106-00228, Revision 5, *Head Loss Calculated Based on Test April 2008*

[27] *Summary of CCI Strainer Head Loss Testing* (May 21, 2015)

[28] Salem Generating Station, Units 1 and 2, *Final Supplemental Response to Generic Letter 2004-02,* dated April 27, 2012, ADAMS Accession Numbers ML12129A388, ML12129A389, and ML12129A390

[29] NEI 04-07, Volume 2 – *Safety Evaluation by the Office of Nuclear Reactor Regulation Related to NRC Generic Letter 2004-02,* Revision 0, December 6, 2004, (NEI 04-07 SER)

[30] NUREG/CR-6808 (LA-UR-03-0880), *Knowledge Base for the Effect of Debris on Pressurized Water Reactor Emergency Core Cooling Sump Performance,* February 2003

[31] NUREG/CR-6772, *GSI-191: Separate-Effects Characterization of Debris Transport in Water*

[32] ANSI/ANS-58.2, *Design Basis for Protection of Light Water Nuclear Power Plants Against the Effects of Postulated Pipe Ruptur,* October 6, 1988

[33] N001-1106-00225, Revision 2, *Evaluation of Effects of Debris on the Palo Verde ECCS Pump Seal Cyclone Separators*

[34] N001-1106-00012, Revision 3, *Palo Verde Sump Debris Downstream Effects Evaluation for ECCS Equipment*

[35] N001-1106-00011, Revision 5, *Palo Verde Units 1, 2, and 3 GSI-191 Down-Stream Effects Debris Ingestion Evaluation*

[36] N001-1106-00013, Revision 2, *Palo Verde Sump Debris Downstream Effects Evaluation for ECCS Valves*

[37] Microtherm Properties Helmut (S+L) + M. Pass (Promat US), Revision 0

[38] Drawing MN106-A00021, Revision 1

[39] LR-N12-0124, Attachment 1 to Salem Nuclear Generating Station Units 1 and 2, Docket Numbers 50-272 and 50-311, *Generic Letter 2004-02 Updated Supplemental Response for Salem*

[40] NRC Letter (ADAMS ML120730181) to NEI, *NRC Review Of Nuclear Energy Institute Clean Plant Acceptance Criteria For Emergency Core Cooling Systems,* dated 2-MAY-2012

[41] 40EP-9EO03, Revision 35, *Emergency Operating Procedure Users Guide*

[42] N001-1106-00247, *Determination of Head Loss Bump-Up Factor For ECCS Strainers,* Revision 0

[43] N001-1106-00223, Revision 3, *Post-LOCA Fuel Deposition Analysis in Support of GSI-191*

[44] WCAP-16793-NP, *Evaluation of Long-Term Cooling Considering Particulate, Fibrous, and Chemical Debris in the Recirculating Fluid*

[45] APS EWR 4746166

[46] APS EWR 4746165

[47] Westinghouse LTR-SEE-16-103, *Evaluation of Debris Concentration in Recirculation Sump Fluid due to a Reactor Vessel Nozzle Break on GSI-191 Ex-Vessel Equipment and Components in the Emergency Core Cooling and Containment Spray Systems for Palo Verde*

[48] N001-1106-00002–DG, Revision 3, (S&L) *Debris Generation Due to LOCA within Containment for Resolution of GSI-191*